

Lawrence Berkeley National Laboratory

Recent Work

Title

I. BETA-SPECTROSCOPIC STUDIES IN THE PROMETHIUM REGION. II. THE CORIOLIS INTERACTION IN DEFORMED NUCLEI

Permalink

<https://escholarship.org/uc/item/3qt1p5nh>

Author

Marshall, Thomas V.

Publication Date

1960-05-01

UNIVERSITY OF
CALIFORNIA

Ernest O. Lawrence

*Radiation
Laboratory*

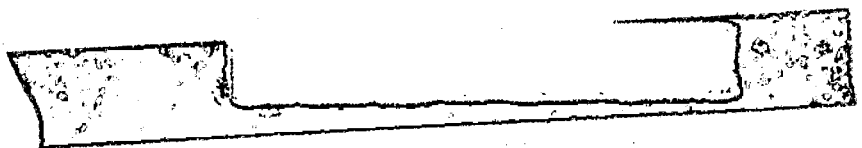
- I. BETA-SPECTROSCOPIC STUDIES IN
THE PROMETHIUM REGION
- II. THE CORIOLIS INTERACTION
IN DEFORMED NUCLEI

TWO-WEEK LOAN COPY

*This is a Library Circulating Copy
which may be borrowed for two weeks.
For a personal retention copy, call
Tech. Info. Division, Ext. 5545*

DISCLAIMER

This document was prepared as an account of work sponsored by the United States Government. While this document is believed to contain correct information, neither the United States Government nor any agency thereof, nor the Regents of the University of California, nor any of their employees, makes any warranty, express or implied, or assumes any legal responsibility for the accuracy, completeness, or usefulness of any information, apparatus, product, or process disclosed, or represents that its use would not infringe privately owned rights. Reference herein to any specific commercial product, process, or service by its trade name, trademark, manufacturer, or otherwise, does not necessarily constitute or imply its endorsement, recommendation, or favoring by the United States Government or any agency thereof, or the Regents of the University of California. The views and opinions of authors expressed herein do not necessarily state or reflect those of the United States Government or any agency thereof or the Regents of the University of California.



UCRL-8740
Chemistry General

UNIVERSITY OF CALIFORNIA
Lawrence Radiation Laboratory
Berkeley, California

Contract No. W-7405-eng-48

- I. BETA-SPECTROSCOPIC STUDIES IN THE PROMETHIUM REGION
- II. THE CORIOLIS INTERACTION IN DEFORMED NUCLEI

Thomas V. Marshall
(Thesis)

May 1960

Printed in USA. Price \$1.75. Available from the
Office of Technical Services
U. S. Department of Commerce
Washington 25, D.C.

Contents

Abstract.	3
Introduction.	4
I. Beta-Spectroscopic Studies in the Promethium Region	6
Experimental Methods.	6
Production of Activities.	6
Chemical Separations.	6
Instruments	9
Samarium-142 and Promethium-142	10
Observation and Mass Assignment of 72-Minute Activity	10
Gamma-Ray Spectrum.	12
Positron Spectrum	14
The Half Life of Promethium-142	14
Discussion.	16
Promethium-149.	26
Gamma-Ray Spectrum.	26
Electron Spectrum	30
Discussion and Decay Scheme	32
II. The Coriolis Interaction in Deformed Nuclei	35
Introduction.	35
The Coriolis Interaction in a General Nucleus	37
The Coriolis Interaction in Protactinium-233 and -231	50
Acknowledgment.	69
References.	70

I. BETA-SPECTROSCOPIC STUDIES IN THE PROMETHIUM REGION
II. THE CORIOLIS INTERACTION IN DEFORMED NUCLEI

Thomas V. Marshall
(Thesis)

May 1960

Lawrence Radiation Laboratory and Department of Chemistry
University of California, Berkeley, California

ABSTRACT

The new isotopes Sm^{142} and Pm^{142} have been produced by the reaction sequence: $\text{Nd}^{142}(\alpha, 4n)\text{Sm}^{142} \xrightarrow{\beta^+, \text{EC}} \text{Pm}^{142}$. The decay characteristics of these isotopes have been determined.

The gamma, beta, and conversion-electron spectra of Pm^{149} have been measured and a decay scheme is proposed for this isotope.

A method for calculating the effect of the Coriolis interaction on the energies of the rotational levels of a generalized, spheroidally deformed nucleus has been developed using a simple nuclear model, and the general effect of this interaction on rotational bands is discussed. Part of the energy level schemes of Pa^{231} and Pa^{233} have been interpreted in terms of rotational bands perturbed by the Coriolis interaction.

I. BETA-SPECTROSCOPIC STUDIES IN THE PROMETHIUM REGION
II. THE CORIOLIS INTERACTION IN DEFORMED NUCLEI

Thomas V. Marshall

(Thesis)

Lawrence Radiation Laboratory, and Department of Chemistry
University of California, Berkeley, California

May 1960

INTRODUCTION

Previous studies of the promethium isotopes have failed to find an activity which could be assigned to mass number 142 although activities have been assigned to all other mass numbers from 141 through 152.¹ Fischer² was able to set the following limits on the half-life of Pm^{142} : 2 minutes $> t_{1/2}$ or $t_{1/2} > 100$ years. Since Pm^{142} must decay to the "magic number" nuclide Nd^{142} it would be expected to have a high decay energy and, unless the decay is highly forbidden, a short half-life. If the half-life of Pm^{142} is very short as Fischer's limit and the expected high decay energy indicate, the most convenient way to study this isotope would be in equilibrium with its parent Sm^{142} . Although Sm^{142} has not been reported in the literature beta-decay systematics indicate that this isotope is probably sufficiently long-lived to be studied directly.

In the present work Sm^{142} has been produced by the reaction $\text{Nd}^{142}(\alpha, 4n)\text{Sm}^{142}$. Promethium-142 has been found to be in equilibrium with it, and the decay characteristics of the two isotopes have been determined.

A marked change in nuclear structure occurs between the isotopes Eu^{151} and Eu^{153} (88 and 90 neutrons respectively). This change is manifested in an abnormally large shift in the nuclear quadrupole moments and in a change in the nuclear energy level structure between the two isotopes. Europium-153 shows a well developed rotational band; there is no readily recognizable rotational structure in Eu^{151} . The second part of this work was undertaken to gain a better understanding of this change.

This problem was approached both experimentally and semi-theoretically. A study of the decays of Pm^{149} and Pm^{151} was made to determine the level structures of Sm^{149} (87 neutrons) and Sm^{151} (89 neutrons) with the hope that this information would give an insight into the nature of this change. A study of the effect of the Coriolis interaction on the rotational bands of deformed nuclei was made to determine if the level structure of Eu^{151} could be explained in terms of rotational bands perturbed by this interaction.

Unfortunately, neither the experimental study of the energy levels of Sm^{149} and Sm^{151} nor the study of the Coriolis interaction has shed any new light on the nature of the sudden change in nuclear structure between the europium isotopes. However, these studies have been fruitful in providing other valuable information. The gamma, beta, and conversion-electron spectra of Pm^{149} are presented here and a decay scheme is given for this isotope.*

A method for calculating the energies of rotational levels perturbed by the Coriolis interaction has been developed using a simple nuclear model, and the general effect of this interaction on rotational bands is discussed. In addition, part of the energy level structures of Pa^{231} and Pa^{233} have been interpreted in terms of rotational bands perturbed by the Coriolis interaction.

*The decay of Pm^{151} will be discussed in a forthcoming UCRL report.

I. BETA-SPECTROSCOPIC STUDIES IN THE PROMETHIUM REGION

EXPERIMENTAL METHODS

Production of Activities

Samarium-142 was produced by bombarding neodymium oxide with alpha-particles in the Berkeley 60-inch cyclotron. The cyclotron targets were prepared in the following manner. Powdered neodymium oxide was suspended in a solution of "Duco" cement in iso-amyl acetate. This slurry was painted onto a 10-mil gold or platinum plate allowing the solvent to evaporate between each layer; the target was flamed periodically to remove all organic matter. A 1-mil cover foil of gold, platinum, or aluminum was placed over the target material and the target was loaded into a "cat's eye" target assembly. The back of the target was cooled with water during the bombardment. The energy of the alpha-particles on the cover foil was 48 Mev.

Promethium-149 was produced by irradiating neodymium oxide enriched in Nd^{148} with slow neutrons in the Materials Testing Reactor at Arco, Idaho, and allowing the Nd^{149} produced by the irradiation to decay to Pm^{149} . The isotopic percentages of the neodymium oxides are given in Table I.

Table I

Isotopic Abundances of Target Neodymium Oxides							
	142	143	144	145	146	148	150
Enriched Nd^{148}	1.60	0.87	5.49	1.05	3.30	84.59	3.10
Natural Neodymium	27.09	12.14	23.83	8.29	17.26	5.74	5.63

Chemical Separations

Two different chemical procedures were used to separate samarium and promethium from the target neodymium and from each other. The first

method, used to separate samarium, is a modification of a procedure developed by Ballou and Newton.³ The procedure is as follows:

1. Dissolve the target in hot 6 N HCl. Add 5 mgs. of Sm^{+3} carrier and precipitate the rare earth hydroxides with NH_3 (or conc. NH_4OH). Centrifuge and wash the precipitate thoroughly with water.
2. Dissolve the precipitate in 6 N HCl. Add an equal amount of 6 N NH_4F to precipitate the rare earth fluorides. Heat for 10 minutes to digest the precipitate, centrifuge, and wash with water.
3. Dissolve the precipitate in conc. HNO_3 saturated with H_3BO_3 . Precipitate the rare earth hydroxides with NH_3 , centrifuge, and wash with water.
4. Dissolve the precipitate in a minimum of 6 N HCl. Transfer to a separatory funnel with 10 ml. of water. Add 8 drops of glacial acetic acid.
5. Add 3 ml. of 0.3% sodium amalgam and shake for 10 seconds. Draw off the Hg layer and save. Repeat 2 or 3 times.
6. Transfer the combined Hg fractions to a second separatory funnel and wash with 30 ml. of water. Repeat the washing in a third separatory funnel.
7. Transfer the Hg layer to a fourth separatory funnel containing 30 ml. of 2 N HCl. Shake until the hydrogen evolution ceases.
8. Withdraw the aqueous layer and precipitate $\text{Sm}(\text{OH})_3$ with conc. NH_4OH . Centrifuge and wash with water.
9. Dissolve the $\text{Sm}(\text{OH})_3$ in acid and evaporate onto counting plates.

Samarium isolated in this manner is reasonably pure if the amount of neodymium is not appreciably greater than the amount of samarium carrier added; if the amount of neodymium is too great there is some carry-over of both it and promethium.* Fluorine-18 also tends to carry through this separation. If its presence is undesirable its concentration may be reduced by further fluoride precipitations.

To isolate promethium activities and to obtain carrier-free samarium activities an ion-exchange column technique was used. For the enriched isotope targets the neodymium oxide was dissolved in hot 12 N HCl, this solution was evaporated to dryness, and the neodymium chloride was redissolved in 0.05 N acid. For the cyclotron targets a rather large amount of acid (6 N HCl) was required to dissolve the target off the backing plate, and to avoid long evaporation times the neodymium was precipitated as the hydroxide, washed, and redissolved in a minimum of 2 N HCl. The dilute acid solutions were loaded onto an ion-exchange column and the rare earths were separated by the method described by Thompson, Harvey, Choppin, and Seaborg.⁴ Dowex-50 was used as the ion-exchange resin and 0.4 M alpha-hydroxyisobutyric acid was used as the eluant. The alpha-hydroxyisobutyric acid was buffered with ammonium hydroxide to give the desired pH; the pH used ranged from 4.1 to 4.8. Since the amount of target material used varied widely, columns of different sizes were used. The columns were operated at a temperature of 87°C.

For samples to be used for the study of beta and conversion-electron spectra the following procedure was used to remove the eluant from the activity. The fraction of the eluant containing the desired activity was acidified to approximately 0.1 N. This solution was passed

* It should be noted that europium is also extracted by the sodium amalgam; it can be separated from samarium by extracting with zinc amalgam (see Reference 3). The zinc amalgam extraction was not necessary for this study since the samples used were not contaminated with europium.

through a small (3 mm. by 2 cm.) Dowex-50 column. The column was washed with 0.05 N acid to remove all of the alpha-hydroxyisobutyric acid and then the activity was stripped from the column with 6 N HCl (or 5 N HNO₃ if the solution was to be evaporated onto aluminum).

Instruments

The energies and intensities of gamma-rays were measured using NaI(Tl) crystals as detectors. The pulses from the photomultiplier tubes coupled to the crystals were analyzed by 50-⁵ and 100-channel⁶ pulse-height analyzers. The NaI(Tl) crystals used were 1-inch by 1-1/2-inches in diameter and 3-inches by 3-inches in diameter bevelled 1/2-inch at an angle of 45°. The observed intensities of the gamma-rays were corrected for crystal efficiency and the Compton effect using the curves of Kalkstein and Hollander⁷ and Heath.⁸ Escape peak corrections were made using the curves of Axel.⁹

Beta spectra were measured with a "lens"-type electron spectrometer of 2% resolution and 2% transmission¹⁰ and a double-focussing electron spectrometer of 0.3% resolution and 0.1% transmission.¹¹ Conversion-electron energies were measured with 130- and 216-gauss permanent magnet electron spectrographs of 0.1% resolution and 0.01 to 0.1% transmission.¹²

Samples for the "lens" spectrometer were prepared by painting 1-mil aluminum foils 2 cm. in diameter with fingernail polish except for an area approximately 2 mm. in diameter in the center. This area was cleaned with insulin and the acid solution containing the activity was evaporated onto it. The samples for the double-focussing electron spectrometer were prepared by evaporating the acid solution of the activity onto strips of 1-mil aluminum or 2-mil copper approximately 1 mm. wide and 5/8 inches long. These samples prepared by evaporation were contaminated with visible mass and gave spectra which were distorted in the low energy region.

The samples for the permanent magnet spectrographs were prepared by electrodepositing the activity as the hydroxide onto 10-mil platinum wires from a 0.1 M ammonium bisulfate solution at a pH of 3.6.

Geiger-Mueller counters and NaI(Tl) detectors coupled to a single channel pulse-height analyzer were frequently used to follow the decay of a sample.

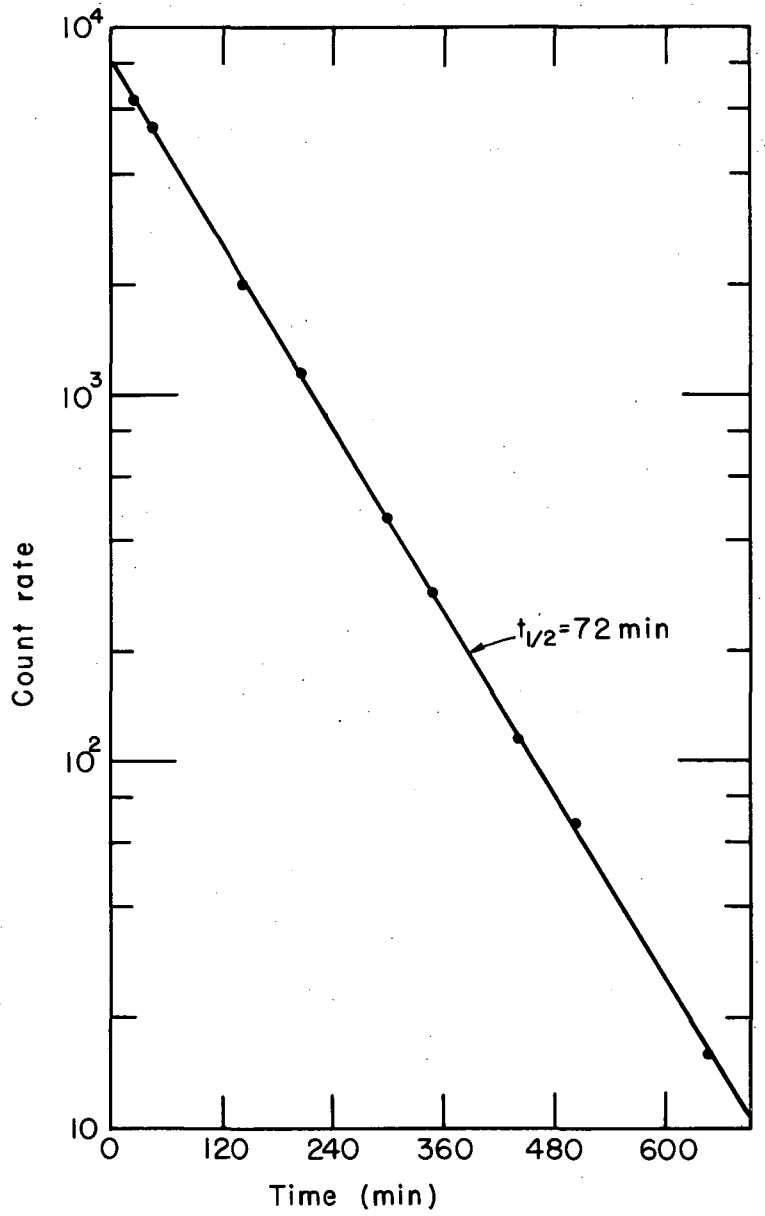
SAMARIUM-142 AND PROMETHIUM-142

Observation and Mass Assignment of 72-Minute Samarium Activity

In the first bombardment of neodymium oxide with alpha-particles the samarium extracted from the target with sodium amalgam showed activities corresponding to 9-minute Sm^{143} , 340-day Sm^{145} , 47-hour Sm^{153} , and a previously unreported activity with a half-life of 80-90 minutes. In later bombardments in which the samarium fraction was separated on an ion-exchange column, the new activity was found to have a half-life of 72 ± 2 minutes (Fig. 1). The longer half-life found in the first bombardment is believed to be due to contamination by F^{18} which carried through the extraction. The 72-minute samarium activity was also found in a single bombardment of Cs_2SO_4 with N^{14} ions.

The 72-minute samarium activity was tentatively assigned to Sm^{142} produced by the reaction $\text{Nd}^{142}(\alpha,4n)\text{Sm}^{142}$. To check this assignment neodymium oxide was bombarded with alpha-particles whose energy (37 Mev) was below the $\alpha,4n$ reaction threshold (39 Mev^{*}). In order to reduce the contamination of the sample by F^{18} , rare earth fluoride precipitations were made both before and after extraction of samarium with sodium amalgam. The annihilation radiation of this sample had a half-life of 115 minutes corresponding to the half-life of F^{18} with no shortening caused by the presence of 72-minute activity. Since in the

* The mass difference computed by Cameron (A Revised Semi-Empirical Atomic Mass Formula, CRP-690, March 1957.) gives a threshold of 39.6 Mev. The subsequently measured positron energies give a threshold of 38.8 Mev.



MU-20257

Fig. 1. Decay curve of the annihilation radiation of Sm^{142} -- Pm^{142} equilibrium mixture.

first bombardment the 72-minute activity predominated even though no special effort was made to eliminate F^{18} , it must be concluded that the 72-minute activity was completely absent or at least greatly reduced in this bombardment. Consequently, the 72-minute activity must be produced by an $\alpha,4n$ reaction since this is the only α, xn reaction whose cross-section would be greatly reduced in going from 44.5 Mev to 37 Mev, and the assignment of the 72-minute activity to Sm^{142} is confirmed.

Di Caporiacco, Ferrero, and Mandò have recently observed a 74-minute activity produced by the irradiation of Sm_2O_3 with bremsstrahlung with a maximum energy of 30.5 Mev. This activity decays by positron emission and K-electron capture. These authors have also assigned this activity to Sm^{142} produced by the $Sm^{144}(\gamma, 2n)Sm^{142}$ reaction.¹³

Gamma-Ray Spectrum

With the exception of the K x-ray peak, Fig. 2 shows the important features of the gamma-ray spectrum of the 72-minute activity; this spectrum was taken using a 1-inch by 1-1/2-inch in diameter NaI(Tl) crystal with beryllium absorbers above and below the sample to annihilate the positrons and a lead absorber above the sample to absorb the K x-rays. The prominent peak at 0.51 Mev is due to the annihilation of the positrons. The small peak at 1.59 Mev decays with approximately the half-life of the annihilation radiation and has been assigned to the 72-minute activity. The intensity of this gamma-ray relative to the number of positrons is 0.24%. The 0.72-Mev peak is probably due to a coincidence between an annihilation quantum and its partner which has been Compton scattered at 180° in the absorber below the sample. The initial half-life of the 1.07-Mev peak is about one-half that of the 0.51-Mev peak indicating that it is due, at least in part, to random coincidences between quanta from separate annihilation events. There may be, however, a contribution to this peak from a gamma-ray of ~ 1.14 Mev with a half-life roughly equal to that of the annihilation radiation.

The ratio of K-electron capture to positron emission for the 72-minute activity has been determined from the corrected relative numbers of K x-rays and annihilation photons to be 1.35 ± 0.15 .

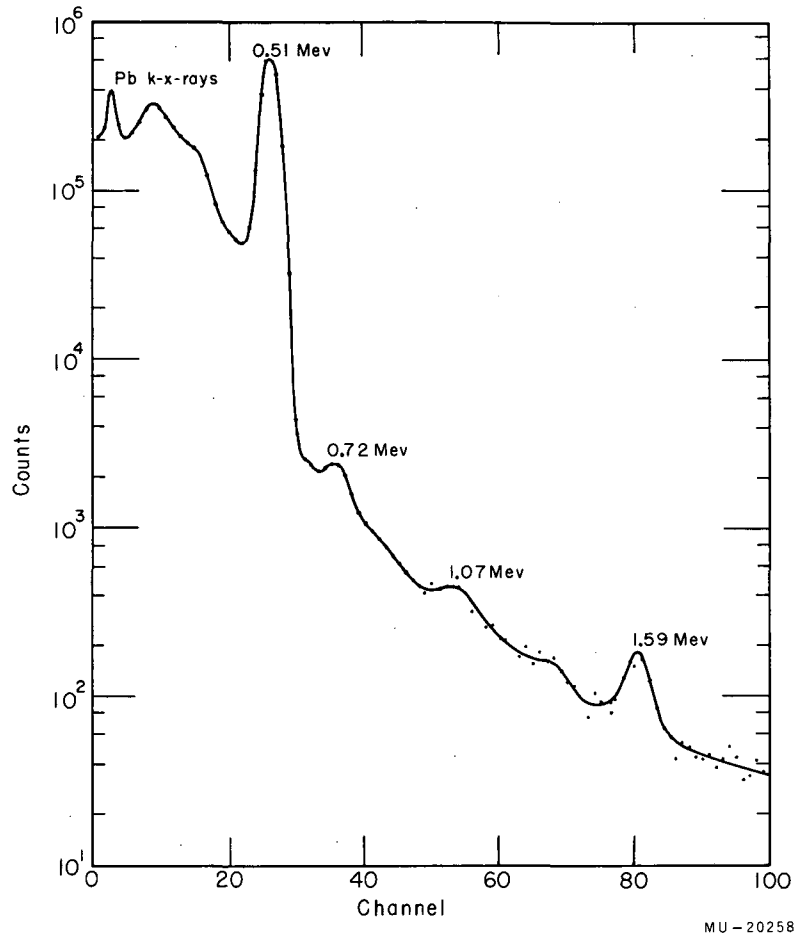


Fig. 2. Gamma-ray spectrum of Sm^{142} -- Pm^{142} equilibrium mixture taken with a 1-1/2-inch by 1-inch NaI(Tl) crystal. Beryllium absorbers were used above and below the sample to annihilate the positrons; a lead absorber was used to remove the K x-rays.

Positron Spectrum

Positron spectra of the 72-minute activity were taken on both the double-focusing and "lens"-type electron spectrometers. Figure 3 shows the Fermi-Kurie plot of the positron spectrum taken on the double-focusing spectrometer.* This plot shows two positron groups with energies of 3.80 ± 0.05 Mev and 1.03 ± 0.07 Mev associated with the 72-minute activity. (The larger limit of error on the low energy side of the 3.8-Mev group is due to uncertainty in the energy calibration of the spectrometer; the spectrum taken on the "lens" spectrometer shows an endpoint of 3.72 Mev for this group.) The relative intensities of the two groups are $87 \pm 2\%$ and $13 \pm 2\%$, respectively.

The Half-Life of Promethium-142

The positron and gamma-ray spectra clearly indicate that Pm^{142} must be in equilibrium with 72-minute Sm^{142} . The presence of two positron groups without a gamma-ray of appropriate energy and abundance to depopulate an excited state populated by the lower energy group shows that there must be two nuclides associated with the 72-minute activity. It would not be expected that the two nuclides are isomers of Sm^{142} since it would be a purely fortuitous circumstance for them to decay with the same half-life. Direct evidence that the second nuclide is Pm^{142} is found in the observation of the low intensity, 1.59-Mev gamma-ray; this energy corresponds to the first excited state (1.57 Mev) of Nd^{142} .¹⁴ Further, the high energy of the one positron group is appropriate to Pm^{142} since its daughter Nd^{142} has a closed shell of 82 neutrons.

Since Pm^{142} is in equilibrium with 72-minute Sm^{142} , its half-life, according to Fischer's limits, must be less than two minutes. A further

* This plot has been constructed using the Fermi function appropriate to promethium decay for the higher energy positron group and the Fermi function appropriate to samarium decay for the lower energy group.

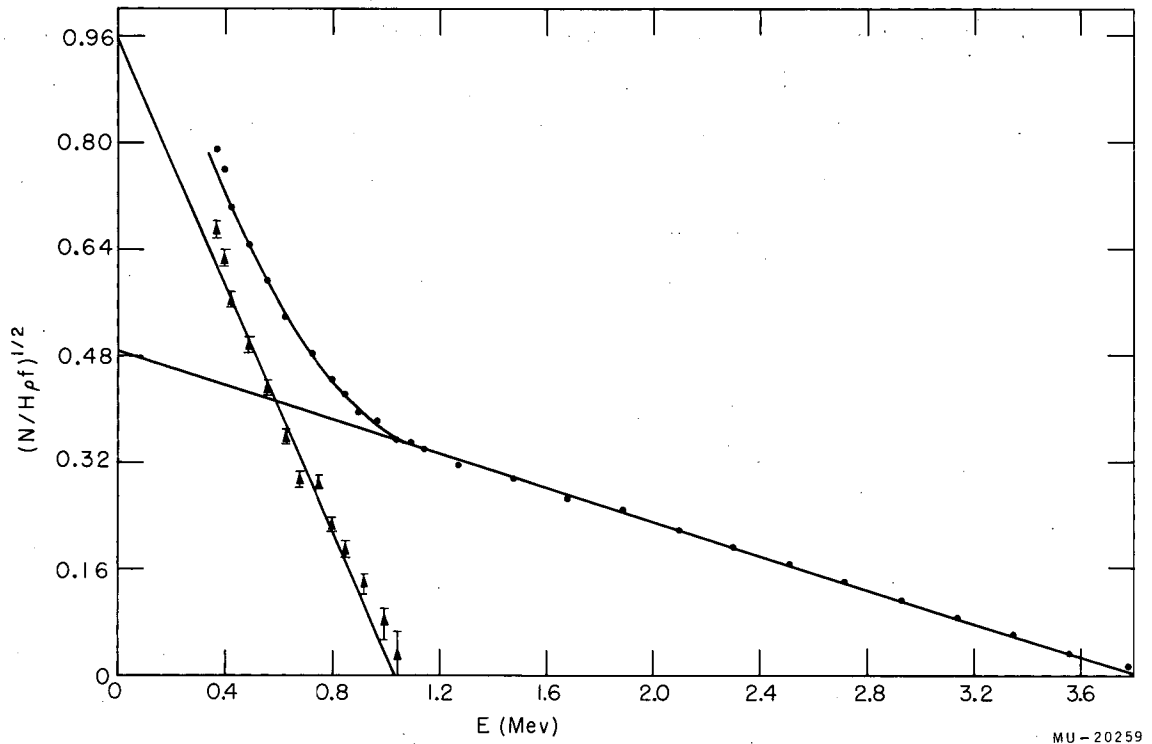


Fig. 3. Fermi-Kurie plot of the positron spectrum of Sm^{142} -- Pm^{142} equilibrium mixture, showing its resolution into components. f for $Z = 60$ was used for the total curve but after the subtraction of the higher energy group, f for $Z = 61$ was used for the lower energy group.

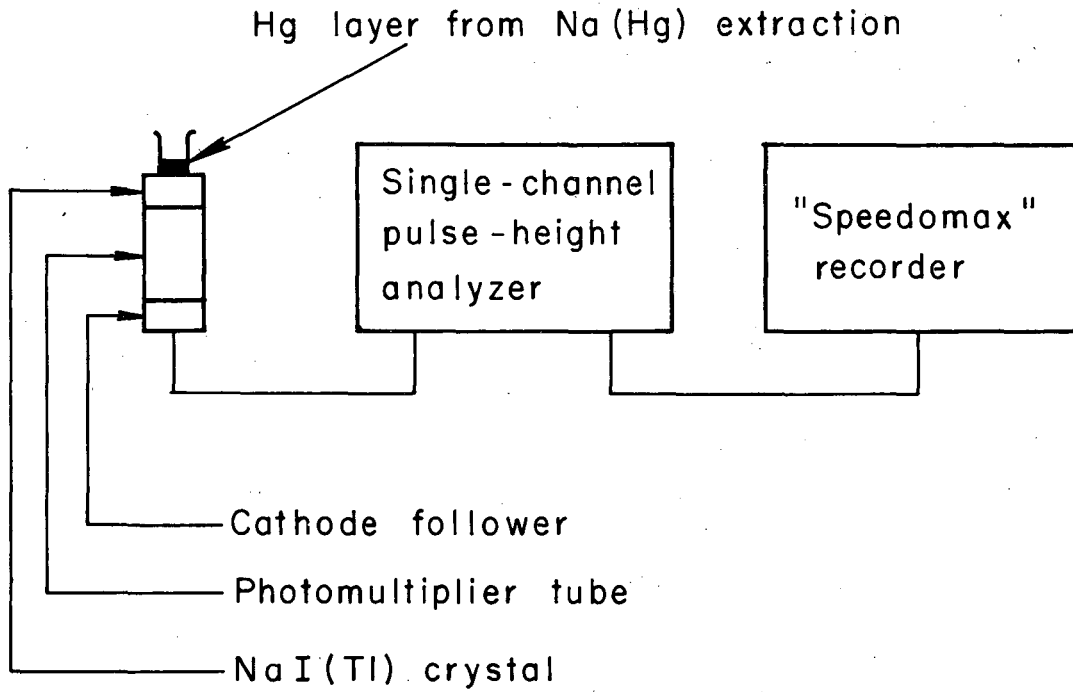
estimate of its half-life was made by assigning the 3.8-Mev positron group to it and assuming that its log ft is similar to those of the similar nuclides Pr^{140} and Eu^{144} ; this estimate placed the half-life between 30 seconds and 2 minutes.

To measure the half-life of Pm^{142} , the following experiment was performed. Samarium-142 was extracted from the equilibrium mixture with sodium amalgam. The mercury layer was immediately withdrawn and placed on a NaI(Tl) scintillation crystal coupled with a photomultiplier tube. The pulses from the photomultiplier tube were passed through a cathode follower and into a single-channel pulse-height analyzer whose "window" was set to accept the annihilation radiation peak. The count rate of the annihilation radiation was recorded with a "Speedomax" recorder operating with a chart speed of six inches per minute. (Figure 4 gives a schematic diagram of the counting arrangement.) In this manner the rate of growth of Pm^{142} into Sm^{142} was determined.

One of the many growth curves obtained is shown in Fig. 5a. Figure 5b is the semi-log plot of (equilibrium count rate - count rate at time t) vs time obtained from this curve; the half-life of Pm^{142} is given directly by the slope of this line. The average value of the half-life obtained from the best growth curves by graphical and least squares analyses is 34 seconds. This value is probably within ± 3 seconds of the true half-life of Pm^{142} .

Discussion

The 3.8-Mev and 1.03-Mev positron groups have been assigned to Pm^{142} and Sm^{142} respectively. The positron, K-electron capture, and L-electron capture branching of the decays of Sm^{142} and Pm^{142} have been calculated from the K-capture to positron ratio, the relative intensities of the positron groups, the genetic relationship between the two isotopes, and the theoretical L- to K-capture ratio ($L/K = 0.13^{15}$). These calculated branching percentages are given in Table II.



MU-20260

Fig. 4. A schematic diagram of the counting arrangement used in measuring the half-life of Pm^{142} .

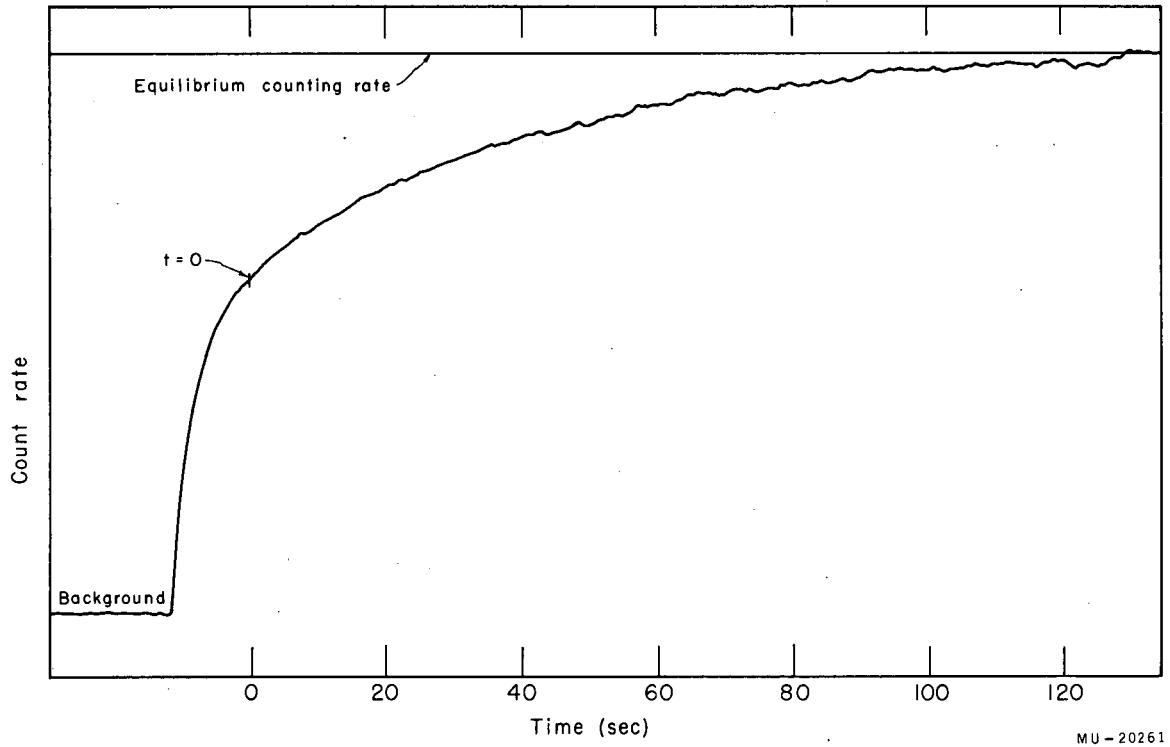
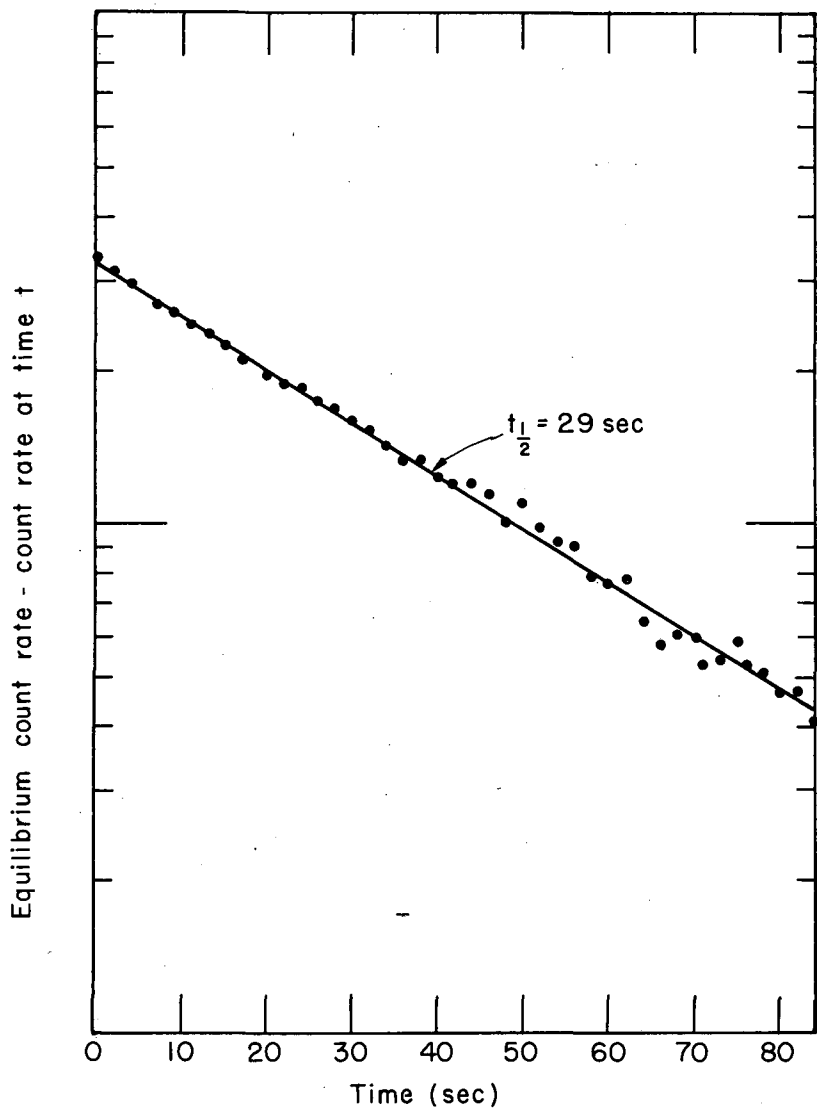


Fig. 5a. Growth curve of Pm^{142} into Sm^{142} .



MU-20262

Fig. 5b. Semi-log plot of (equilibrium count rate - count rate at time t) vs time. The half-life of Pm^{142} is given directly by the slope of this line. (A constant equilibrium count rate was assumed in constructing this curve; when the 72-minute decay of the equilibrium count rate is considered, the half-life is increased about 4 seconds.)

Table II

Branching in the Decays of Sm^{142} and Pm^{142}		
	Sm^{142}	Pm^{142}
K-Electron Capture:	79%	27%
L-Electron Capture:	10%	4%
Positron Emission:	10%	69%

The 1.59-Mev gamma-ray has been assigned to the transition from the 1.57-Mev excited state of Nd^{142} to the ground state. The abundance of population of this excited state by Pm^{142} decay is 0.2%.

The experimental branching percentages predict that the ratio of promethium K x-rays (samarium K-EC) to neodymium K x-rays (promethium K-EC) should be 2.9 in the equilibrium mixture. To measure this ratio experimentally a critical x-ray absorption experiment was performed. Due to the fairly rapid decay of the sample the absorption curve was not carried out to high absorber thicknesses. Unfortunately, the low absorber part of the curve is not very sensitive to the ratio promethium K x-rays/neodymium K x-rays, and a direct determination of this ratio could not be obtained from the absorption curve. Consequently, absorption curves for the ratios 2.5, 2.9, and 3.5 were constructed using the half-thicknesses* in barium (powdered $\text{Ba}(\text{C}_2\text{H}_3\text{O}_2)_2$ was used as the absorber) and the relative intensities of the various K x-rays. These curves are

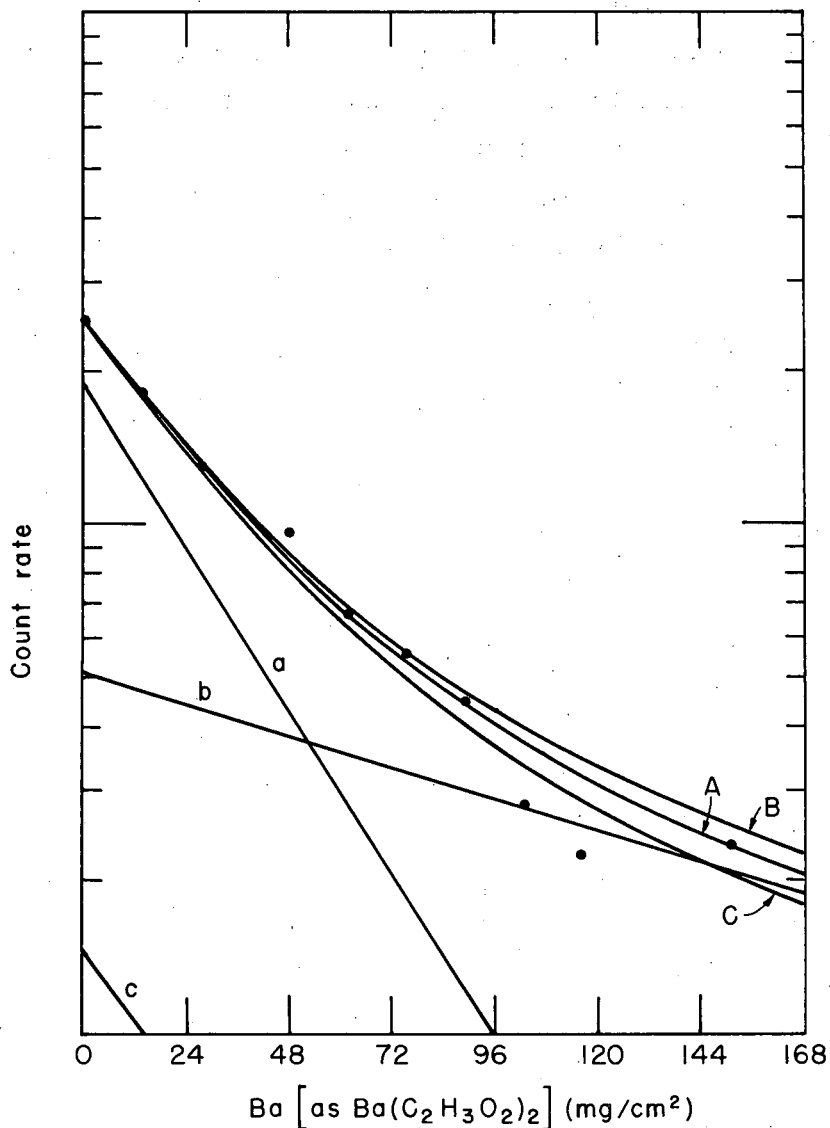
* These half-thickness values were obtained by graphically extrapolating, in analogy to the data of Grodstein¹⁶ for x-ray absorption in tin, iodine, and tungsten, the absorption coefficient of barium at 102 kev given by Davisson and Evans.¹⁷ The ratio of the absorption coefficient just above the K edge to that just below it was taken to be equal to the ratio of the K to L_I electron binding energies. These extrapolated values gave better agreement with the experimental data than those obtained from absorption coefficient data for barium given by S. J. M. Allen.¹⁸

compared to the experimental data in Fig. 6. This comparison shows that the ratio samarium K-EC/promethium K-EC = 2.9 is consistent with the experimental data and that the most probable value of this ratio is between 2.7 and 3.0.

The log ft values of the observed transitions are: from Sm^{142} to the ground state of Pm^{142} -- log ft=5.1; from Pm^{142} to the ground state of Nd^{142} -- log ft=4.3; from Pm^{142} to the 1.57-Mev level of Nd^{142} -- log ft=6.2. The log f values used are those of Feenberg and Trigg.¹⁹ $\log f = \log (f_{\beta^+} + f_K)$ was used in conjunction with the partial half-life for ($\beta^+ + K$) decay to minimize the dependence of log ft on the branching ratio.

The log ft values of the transitions to the ground states of Pm^{142} and Nd^{142} indicate that these transitions are allowed. This limits the possible spin assignments for Pm^{142} to either 0+ or 1+. The spin of the 1.57-Mev level of Nd^{142} has been previously assigned as 2+.^{14,20} The log ft value of 6.2 for the transition to this level is much too low for a second forbidden transition. Thus, the 0+ spin assignment is ruled out and the spin of Pm^{142} must be 1+. This is in agreement with Fischer's postulate² that the odd neutron should be in a $d_{3/2}$ state, the odd proton in a $d_{5/2}$ state with coupling, according to Nordheim's rules, to give a spin of 1+.

The transition to the first excited state of Nd^{142} , although allowed, has an ft value 80 times greater than the ft of the ground state transition. If it is assumed that the decay to the ground state goes to a configuration of two $d_{3/2}$ neutrons coupled to give $I = 0$ and the decay to the excited state goes to a configuration of two $d_{3/2}$ neutrons coupled to $I = 2$, Rose and Osborn's²¹ formulation for the beta-decay matrix elements of the two nucleon configurations predicts that the ft of the transition to the excited state should be 50 times that of the ground state transition. Although this is quite good agreement, it may perhaps be improved by considering an admixture of a $(d_{5/2} p)_{I=2}^2$ configuration in the excited state. It should be noted, however, that the Rose and Osborn formulation gives rather poor agreement with experiment in many



MU-20263

Fig. 6. Critical absorption curves for the K x-rays of Sm^{142} -- Pm^{142} equilibrium mixture. \odot experimental points. Curves A, B, and C are constructed for promethium K x-rays/neodymium K x-rays = 2.9, 2.5, and 3.5 respectively. Curves a, b, and c are, respectively, the contributions of promethium $\text{K}\alpha$ and $\text{K}\beta$ x-rays, neodymium $\text{K}\alpha$ x-rays, and neodymium $\text{K}\beta$ x-rays to curve A. For curves a, b, and c weighted averages were used for $d_{1/2}$'s; for curves A, B, and C individual $d_{1/2}$'s were used.

cases of similar decays. The excellent agreement obtained here may be due to the fact that Nd^{142} is a closed-shell nucleus.

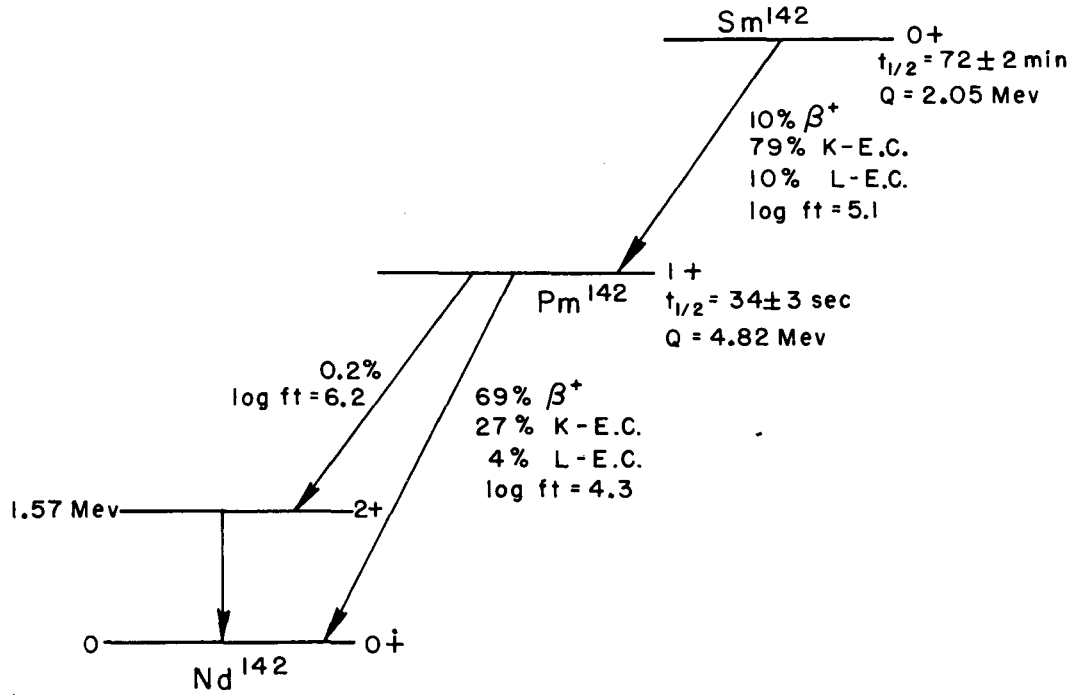
The experimentally measured K-capture/positron ratios are compared in Table III to the theoretically predicted ratios. The uncertainties in the experimental ratios are derived from the uncertainties in the relative positron intensities and the K-electron capture/positron ratio of the equilibrium mixture with the additional restraint that the ratio promethium K x-ray/neodymium K x-rays = 2.9 ± 0.2 . The theoretical ratios are interpolated from the values given by Zweifel.²² The uncertainties given for the theoretical ratios correspond to the uncertainties in the measured positron energies.

There are clearly discrepancies between the experimental and theoretical ratios with the experimental ratio being larger than the theoretical ratio in the decay of Pm^{142} and smaller in the decay of Sm^{142} . In contrast to these discrepancies, Perlman, Welker, and Wolfsberg²³ found fairly good agreement between experimental and theoretical K-capture/positron ratios for a number of allowed transitions in low and medium weight nuclei. However, the one clear case of disagreement which they found was the decay of Sn^{111} which had both the highest Z (50) and the highest positron energy ($E_{\text{max}} = 1.51 \text{ Mev}$) of the nuclei considered.

The decay scheme for the chain $\text{Sm}^{142} \rightarrow \text{Pm}^{142} \rightarrow \text{Nd}^{142}$ is given in Fig. 7. The decay of Pr^{140} ,²⁴ which is just two protons removed from Pm^{142} , is nearly identical to that of Pm^{142} . The two decay schemes are compared in Fig. 8.

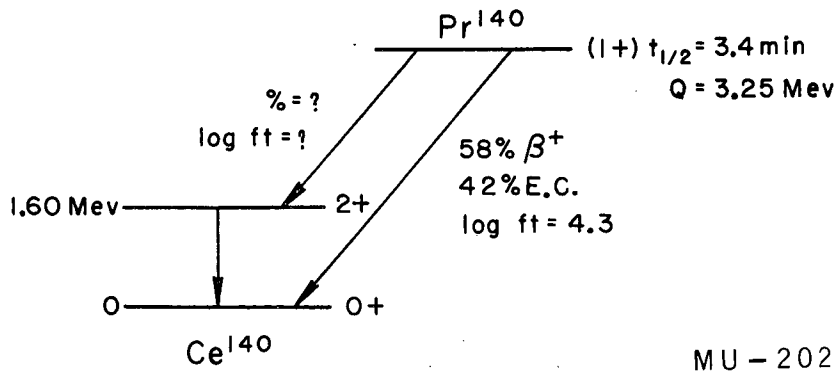
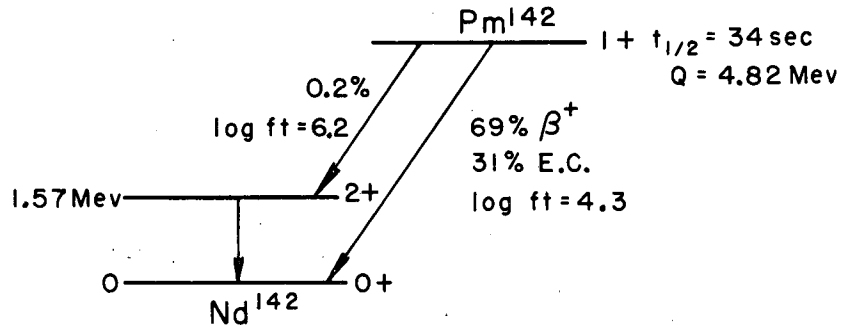
Table III

	K/ β^+ Ratios	
	Experimental	Theoretical
Sm^{142}	8 ± 2	15 ± 3
Pm^{142}	0.40 ± 0.06	0.23 ± 0.02



MU-20264

Fig. 7. Decay scheme of Sm^{142} -- Pm^{142} -- Nd^{142} decay chain.



MU - 20265

Fig. 8. Comparison of Pm¹⁴² and Pr¹⁴⁰ decay schemes.

PROMETHIUM-149

The decay of Pm^{149} has been studied previously by several experimenters. Their studies have shown that Pm^{149} decays with a half-life of about 50 hours by the emission of β^- -particles with a maximum energy of about 1 Mev and there is a prominent 285-keV gamma-ray in coincidence with the beta-particles.²⁵ The results of the present study agree with these observations, and in addition, several new features of the decay of Pm^{149} have been found.

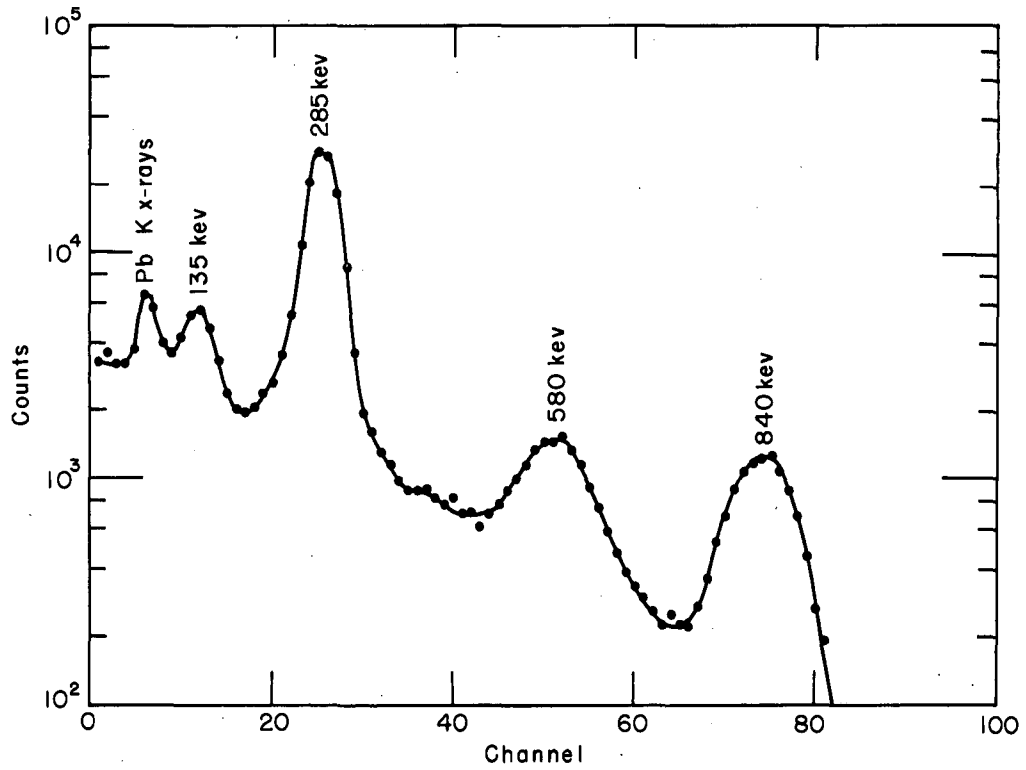
Gamma-Ray Spectrum

The gamma-ray spectrum of Pm^{149} is shown in Fig. 9. This spectrum was taken using a 3-inch by 3-inch, bevelled NaI(Tl) crystal and 4 grams/cm² of lead absorber. The 285-keV peak has a 53 hour half-life and corresponds to the prominent gamma-ray previously reported. The 840-keV peak also has a 53 hour half-life and is assigned to the decay of Pm^{149} . The 135-keV peak decayed at the same rate as the 285-keV peak. However, its energy corresponds to the energy of a 285-keV photon Compton scattered at 180° and it is assigned as the "backscatter" peak of the 285-keV gamma-ray rather than as a gamma-ray associated with the decay of Pm^{149} .

The 580-keV peak initially decayed at about the same rate as the 285- and 840-keV peaks indicating that there is a 580-keV gamma-ray associated with Pm^{149} decay. After a few days its decay rate appeared to be slower and the peak shifted to lower energies. This is probably due to a slight contamination of the sample by 11-day Nd^{147} which has a prominent 532-keV gamma-ray.²⁵

After subtracting the contribution of Nd^{147} to the 580-keV peak, the relative intensities of the 285-, 580-, and 840-keV gamma-rays are 100, 5, and 6 respectively.

The approximately 1-MeV gamma-ray reported by Fischer²⁶ may correspond to the 840-keV gamma-ray observed here. The 1.3 ± 0.2 -MeV gamma-ray reported by Rutledge, Cork, and Burson²⁷ was not observed; the upper limit of its possible intensity is 0.1 (on the relative intensity scale used above).



MU-20266

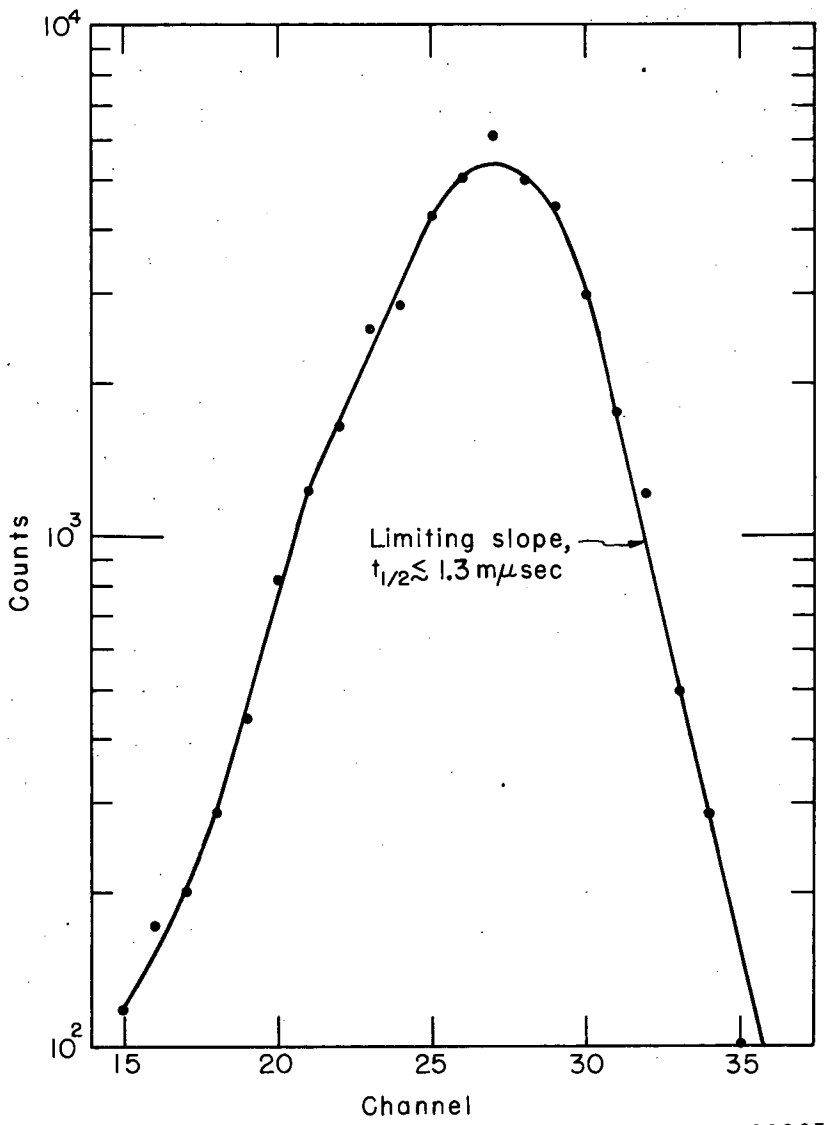
Fig. 9. Gamma-ray spectrum of Pm^{149} taken with a 3-inch by 3-inch NaI(Tl) crystal and a 4 gm/cm^2 lead absorber.

Gamma-gamma coincidence studies were made using the coincidence unit of the 100-channel pulse-height analyzer (Penco). The energy of the gate pulse was selected by a single-channel pulse-height analyzer. These studies showed that there are no coincidences between the 285-, 580-, and 840-keV gamma-rays.

The absence of gamma-gamma coincidences unambiguously establishes excited levels in Sm^{149} at 285, 580, and 840 keV. The energies of possible transitions between these levels are 260, 295, and 555 keV. These energies are such that the corresponding gamma-rays would not be resolved from the 285- and 580-keV gamma-rays in the singles spectrum. However, the coincidence data enable us to set an upper limit on the intensity of these gamma-rays of approximately 10% of the intensity of the 580-keV gamma-ray.

In addition to the gamma-gamma coincidence studies, beta-gamma delayed coincidence measurements were made to determine the lifetime of the 285-keV level of Sm^{149} . The time delay between the beta-particle and the coincident gamma-ray was converted into a pulse-height²⁸ and the pulses were analyzed with a 50-channel pulse-height analyzer. Each channel represents an increment of time and the counts recorded in the channel gives the number of events having a time delay within this increment. When a time-delay spectrum obtained in this manner is plotted on a semi-log scale the slope of the upper side of the curve gives the half-life of the state being studied.

The delay curve for the 285-keV level of Sm^{149} is shown in Fig. 10. For this curve each channel corresponds to a time increment of 1.13×10^{-9} seconds. The slope of this delay curve gives a half-life of 1.3×10^{-9} seconds; however, this corresponds to the limiting half-life which can be measured by the experimental procedure employed and 1.3×10^{-9} seconds is only an upper limit on the half-life of the 285-keV level of Sm^{149} .



MU-20267

Fig. 10. β^- -- 285-kev gamma delay curve. 1.3×10^{-9} seconds is the upper limit on the half-life of the 285-kev level of Sm^{149} .

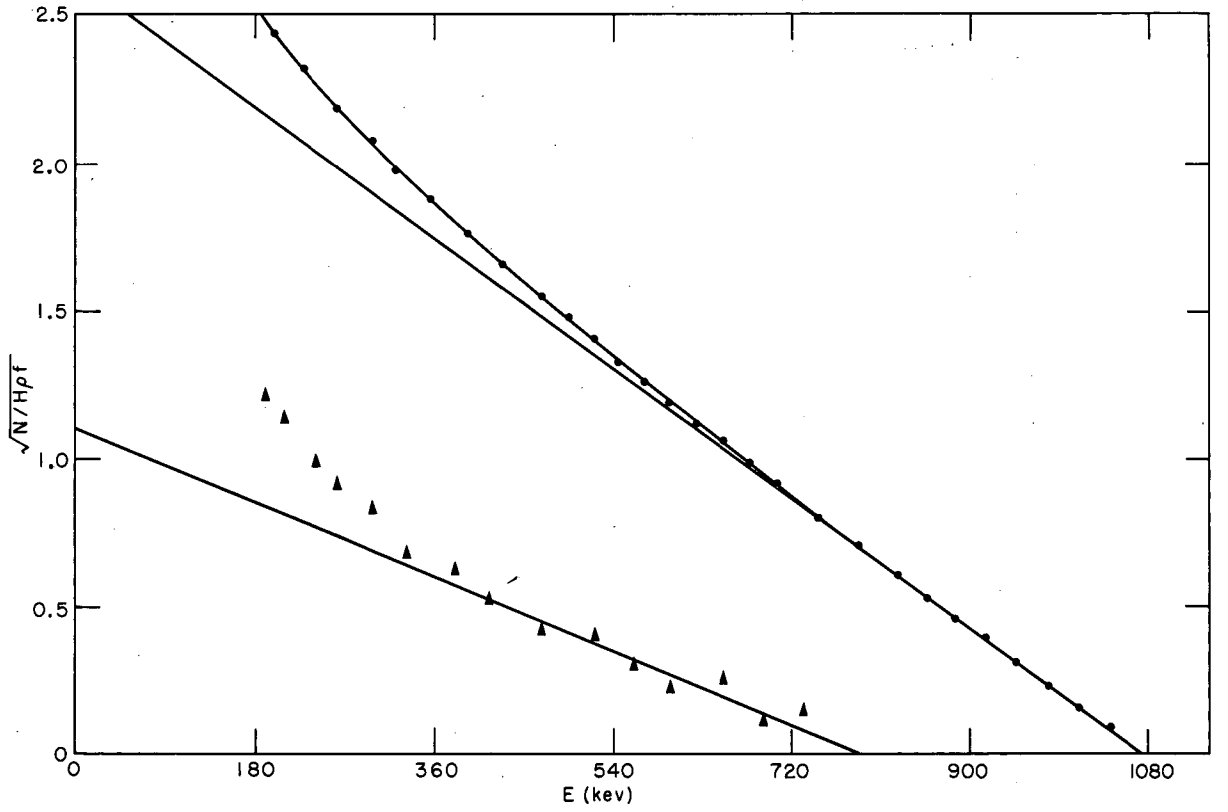
Electron Spectrum

The beta spectrum of Pm^{149} was measured with the double-focusing electron spectrometer. The Fermi-Kurie plot of this spectrum is shown in Fig. 11. The curvature of this plot indicates that the spectrum is complex but it is difficult to resolve the spectrum unambiguously. However, the gamma-ray data show that the highest energy beta group must populate either the ground state or the 285-keV level of Sm^{149} . Since the energy difference between the 285- and 580-keV levels is 295 keV, it seems reasonable that the spectrum should initially be resolved into two components with an energy separation of ~ 290 keV. This resolution is shown in Fig. 11. The energies of the two beta groups are 1.07 ± 0.02 MeV and 0.79 MeV and their intensities are 90% and 10% respectively. The continued curvature of the spectrum probably is due mostly to sample thickness rather than to a third resolvable beta group.

The conversion-electron lines of the 285-keV transition were studied using the 130-gauss permanent magnet spectrograph. The data obtained are summarized in Table IV. These lines are superimposed on an intense beta background and it was not possible to obtain relative intensities from densitometer measurements. The K/L_I ratio determined from visual comparison may easily be in error by as much as 50%. The transition energy of 285.6 keV and the K/L_I ratio of 6 agree within experimental errors with the transition energy of 284.9 keV and K/L ratio of 8.0 ± 2.5 reported by Rutledge, et al.²⁷

Table IV

Conversion-Electron Lines of Pm^{149}			
E_{e^-} (keV)	Visual Intensity	Assignment	Transition Energy (keV)
238.7	14	K	285.6
278.0	2.3	L_I	285.7
283.7	weak	$M_{(I)}$	285.4



MU-20268

Fig. 11. Fermi-Kurie plot of the beta spectrum of Pm^{149} , showing its resolution into components.

Discussion and Decay Scheme

Excited levels in Sm^{149} at 285, 580, and 840 keV have been established by the gamma-ray data. The energy difference between the two beta groups may correspond either to the energy separation of the ground and first excited states or the separation of the first and second excited states. However, the relative intensities of the beta groups are a factor of two different from the relative intensities of the 285- and 580-keV gamma-rays. For this reason, it seems probable that the higher energy beta group populates the ground state and the lower energy group populates the 285-keV level.

Using these assignments, the intensities and the log ft values of the transitions to the ground, 285-, 580-, and 840-keV states can be calculated. These values are given in Table V.* The log ft values indicate that these transitions are all first forbidden, i.e., $\Delta I = 0, \pm 1$ with a change of parity. If these classifications are correct, all of these levels would then have the same parity and the maximum spin difference between them would be two.

Table V

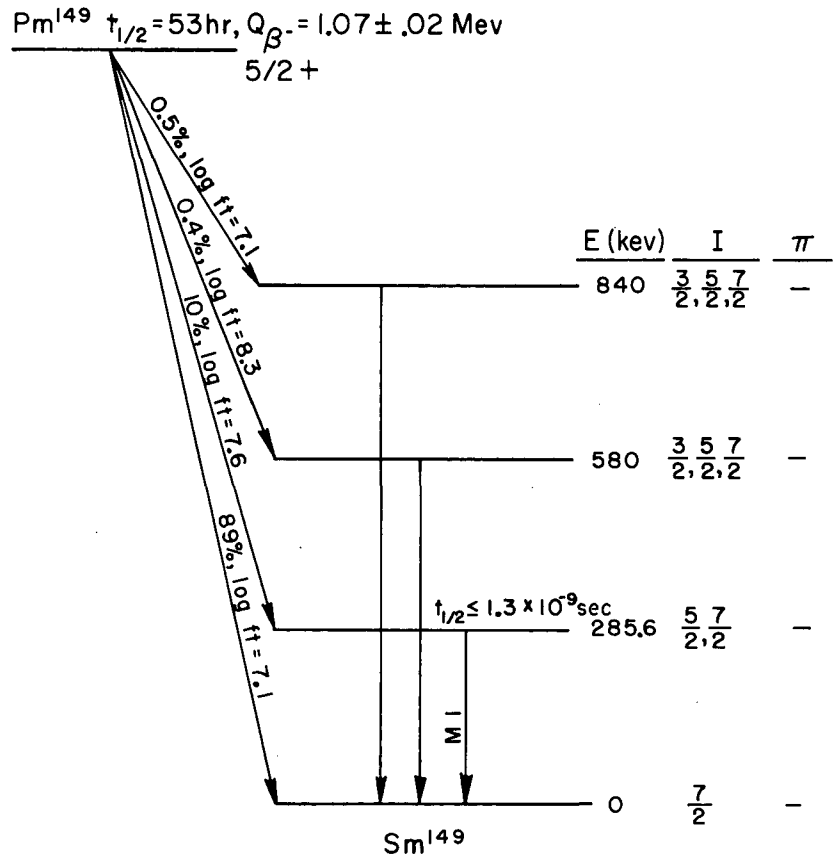
Intensities and Log ft's of the Beta Transitions of Pm^{149}			
Level Populated	E_{β} (keV)	Intensity (%)	log ft
ground	1070	89	7.1
285-keV	790	10	7.6
580-keV	490	0.4	8.3
840-keV	230	0.5	7.1

*The intensities of the transitions to the 580- and 840-keV levels have been corrected for the internal conversion of the 285-keV transition using the M1 conversion coefficients for this transition.

The 285-keV transition has been assigned by Rutledge, et al.²⁷ as a magnetic-dipole transition. The data obtained in this study support this assignment. The spin and parity limitations implied by the beta-transition classifications limit the possible multipolarities of this transition to M1 and E2. The theoretical K/L_I ratios for M1 and E2 are 7.4 and 9.3 respectively.²⁹ The K/L_I ratio of 6 determined here is in better agreement with an M1 assignment than with an E2 assignment. Further, the absence of the L_{II} and L_{III} conversion lines is consistent with an M1 assignment but is not consistent with an E2 assignment.

It is difficult to interpret the levels of Sm^{149} in terms of a nuclear model since it lies between the regions of applicability of the shell model and the strong coupling, collective model. However, the ground state spins and parities of Sm^{149} and Pm^{149} may be interpreted in terms of the shell model predictions. The measured spin of Sm^{149} is $7/2$.^{30,31} This would correspond to the odd neutron being in an $f_{7/2}$ orbital. As pointed out in the discussion of the Pm^{142} ground state spin, the odd proton of promethium would be expected to be in a $d_{5/2}$ orbital. The transition between ground states would then be a $\Delta I = 1$, yes transition in agreement with the experimental log ft. (These assignments have previously been given by Feenberg.³²)

The results of this study of the decay of Pm^{149} are summarized in the decay scheme shown in Fig. 12. This decay scheme is nearly identical to that proposed by Burson and Schmid.³³ However, they have chosen to classify the beta transition to the 580-keV level as a $\Delta I = 2$, yes transition while we prefer the $\Delta I = 0, \pm 1$, yes classification. They also observed a 548-keV gamma ray in coincidence with the 285-keV gamma ray. This observation is not in conflict with the absence of coincidences reported here since their coincidence circuit had a much smaller resolving time³⁴ than the coincidence circuit used in this study and would be more sensitive for the detection of low intensity coincidences.



MU - 20269

Fig. 12. Decay scheme of Pm^{149} .

II. THE CORIOLIS INTERACTION IN DEFORMED NUCLEI

INTRODUCTION

In their limiting solution for the strong coupling of individual nucleonic motion to the collective motions of a spheroidally deformed nucleus Bohr and Mottelson³⁵ treated the motion of the individual nucleons as being separable from the collective motions. In actual practice, however, this separation will never be complete. One of the interactions which couples the nucleonic and collective motions, causing a breakdown in this adiabatic approximation, is due to the Coriolis force exerted on the individual nucleons by the rotational motion of the nucleus. This present work will consider the effect of this interaction on the energy spacing of the levels in the rotational bands predicted by the strong coupling model.

In the strong coupling model with the adiabatic approximation the energies of the levels in a rotational band are given by

$$E_I = E_0 + \frac{\hbar^2}{2\mathcal{I}} I(I+1) \quad (1)$$

where E_I is the energy of the level with spin I , E_0 is a constant, and \mathcal{I} is the moment of inertia. In order for the adiabatic approximation to be valid, it is necessary that the frequency of particle excitations be much greater than the frequency of collective excitations. This condition is generally met in the highly deformed nuclei in the mass regions of $A \sim 25$, $155 < A < 190$, and $A > 230$, and this model has been highly successful in interpreting nuclear spectra in these regions. However, even in these regions the experimental nuclear spectra are often found to deviate slightly from the simple rotational spectra described by Equation (1). Therefore, one interest in the study of the Coriolis interaction in deformed nuclei is that it may provide an explanation of many of these small deviations in rotational structure.

Also, in these regions of large deformation, we may find some nuclei which have interacting particle states with a relatively small energy separation, and for these the adiabatic approximation will no

longer be valid. Further, we must expect this approximation to fail near the edges of these regions, since, as the nuclear deformation decreases, the rotational excitation frequency will increase and the particle excitation frequency will decrease. We may hope, then, that by including the effect of the Coriolis interaction we may extend the strong coupling model to these nuclei and explain their spectra in terms of admixed rotational bands.

The first part of this present work gives a development of the Coriolis interaction in a generalized nucleus which enables us to predict, in a qualitative manner, the effect of this interaction upon the rotational energy level spacings. The second part is a more detailed application of the Coriolis interaction to the energy levels of Pa²³¹ and Pa²³³.

This interaction has been previously considered by Bohr,³⁶ Rasmussen,³⁷ and, in greater detail, by Kerman.³⁸ (Bohr has designated the Coriolis operator as U_1 ; Kerman calls the interaction "rotational particle coupling" or RPC.) Before proceeding to the development of this interaction in a general nucleus, we give here a summary of the observations of these authors concerning its properties and effects.

The Coriolis interaction couples states which have the same spin and parity but differ by one in K and Ω , the projections of the nuclear spin \vec{I} and the particle angular momentum \vec{j} on the nuclear symmetry axis. The strength of the interaction increases with increasing j and increasing I . The interaction will be most important in odd-mass nuclei since they will have lower-energy excited particle states. (This work will consider only odd-mass nuclei and low energy rotational bands for which $K = \Omega_k$)

If the interaction is small, its effect on the energy levels of the lower energy rotational band may be manifested only in an increase in the moment of inertia. Prior³⁹ has successfully correlated the increase in momenta of inertia in going from an even-even nucleus to the next heavier odd A nucleus with the effect of the Coriolis force on the odd nucleon. In addition to the increase in the moment of inertia this

band may show an $I^2 (I + 1)^2$ energy correction term of either sign. It should also be noted here that the upper of two interacting bands will have an apparent decrease in the moment of inertia. If the interaction is large, compared to their separation, the rotational bands may be so distorted that they will not be recognizable as such.

In addition to the energy effects noted above, the mixing of levels may have marked effects on properties which are sensitive to the nuclear wave function such as magnetic moments and electromagnetic transition probabilities. Kerman³⁸ has given formulae for the electromagnetic transition probabilities between admixed states.

THE CORIOLIS INTERACTION IN A GENERAL NUCLEUS

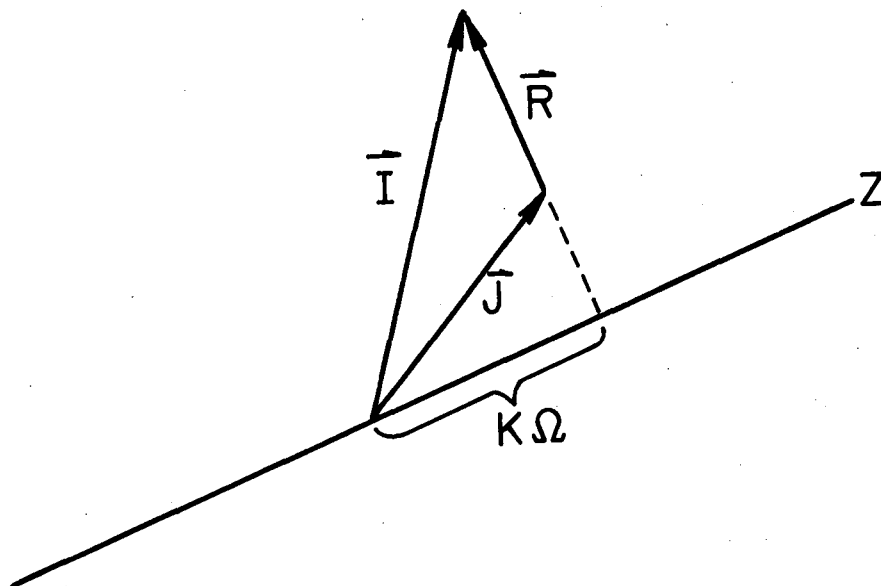
To calculate the effect of the Coriolis interaction in a general nucleus we will use a nuclear model like that of Nilsson⁴⁰ in which the $(2j + 1)$ -degenerate, closed-shell orbitals are split, under the influence of an axially symmetric, non-spherical potential, into $(j + 1/2)$ doubly-degenerate orbitals characterized by Ω , the projection of \vec{j} on the nuclear symmetry axis. The appropriate nuclear wave functions are of the form given by Bohr and Mottelson:³⁵

$$\bar{\Psi} = \varphi \left\{ \chi_{\Omega} D_{MK}^I + (-)^{I-j} \chi_{-\Omega} D_{M-K}^I \right\} .$$

φ and D describe the vibrational and rotational motion of the nucleus and χ the individual nucleonic motion.

If we consider a nucleus composed of a "core" of paired nucleons plus one nucleon which has a different \vec{j} than any of the like nucleons in the "core", the coupling of its angular momenta will be as shown in Fig. 13. \vec{I} , \vec{j} , and \vec{R} are, respectively, the total nuclear, the particle, and the rotational angular momenta; K and Ω are the projections of \vec{I} and \vec{j} on the nuclear symmetry axis z . For this nucleus

$$\langle R^2 \rangle = \langle (\vec{I} - \vec{j})^2 \rangle = I(I + 1) + j(j + 1) - 2\vec{I} \cdot \vec{j} .$$



MU - 20270

Fig. 13. Vector diagram of the coupling of the angular momenta of a spheroidally deformed nucleus.

We are, however, interested in the more general case in which we have \underline{n} nucleons with the same \vec{j} outside of the "core". For this case

$$\begin{aligned} \langle R^2 \rangle &= \langle (\vec{I} - \vec{j}_1 - \vec{j}_2 \dots - \vec{j}_n)^2 \rangle \\ &= I(I+1) + nj(j+1) - 2 \sum_{i=1}^n \vec{I} \cdot \vec{j}_i + 2 \sum_{\substack{i,k=1 \\ i \neq k}}^n \vec{j}_i \cdot \vec{j}_k. \end{aligned}$$

Since we are interested in odd-A nuclei, we will consider only odd \underline{n} .

We now wish to evaluate that part of $\langle R^2 \rangle$ which is diagonal in K and Ω . For this evaluation we will assume that only one nucleon is unpaired; that is, the \underline{n} nucleons fill into the appropriate orbitals in pairs leaving only the odd nucleon unpaired. Then

$$- 2 \sum_{i=1}^n \vec{I} \cdot \vec{j}_i = - 2 K \Omega_p - 2 (I_x j_{px} + I_y j_{py})$$

where the subscript p refers to the unpaired nucleon. The second term on the right side is the Coriolis operator and makes no diagonal contribution unless $K = 1/2$ in which case there is a diagonal contribution of

$$(-)^{I+j} (j + 1/2) (I + 1/2).$$

Rewriting the terms $\vec{j}_i \cdot \vec{j}_k$ we have

$$\begin{aligned} \vec{j}_i \cdot \vec{j}_k &= j_{iz} j_{kz} + j_{ix} j_{kx} + j_{iy} j_{ky} \\ &= \Omega_i \Omega_k + 1/2 (j_{i+} j_{k-} + j_{i-} j_{k+}) \end{aligned}$$

where $j_{\pm} = j_x \pm ij_y$. The term $(j_{i+} j_{k-} + j_{i-} j_{k+})$ leads to an exchange of nucleons if $\Omega_i = \Omega_k \pm 1$. Because the wave function is anti-symmetric in the exchange of nucleons, these terms enter with a sign change. The contribution of these exchange terms can be evaluated using the relations

$$j_+ x_\Omega = [j(j+1) - \Omega(\Omega+1)]^{1/2} x_{\Omega+1}$$

$$j_- x_{\Omega+1} = [j(j+1) - \Omega(\Omega+1)]^{1/2} x_\Omega$$

Combining the individual terms, we have

$$\begin{aligned} \langle R^2 \rangle_{\text{diag}} &= I(I+1) + n j(j+1) - 2K\Omega_p \\ &+ (-)^{I+j} (j+1/2)(I+1/2) \delta_{K,1/2} \\ &+ 2 \sum_{\substack{i,k=1 \\ i \neq k}}^n \Omega_i \Omega_k - \sum_i [j(j+1) - \Omega_i(\Omega_i+1)] \end{aligned} \quad (2)$$

where the last sum is taken over all the i (th) nucleons (outside of the "core") for which there is a k (th) nucleon (outside of the "core") such that $\Omega_i = \Omega_k - 1$. The diagonal contribution to the rotational energy is

$$E_R(\text{diag}) = \frac{\hbar^2}{2\mathfrak{I}} \langle R^2 \rangle. \quad (3)$$

This is just the familiar formula for the energies of unperturbed rotational levels since, for a given configuration of n nucleons, all of the terms of $\langle R^2 \rangle$ are independent of I except

$$I(I+1) + (-)^{I+j} (j+1/2)(I+1/2) \delta_{K,1/2}.$$

However, we have an explicit expression for that part of the rotational energy which is independent of I .

In order to calculate the effect of the Coriolis interaction on the rotational levels given by Eq. (3) we need to know the energy separation between the different particle states (i.e., the different possible configurations of the n nucleons). For this calculation we will assume that the relative energies of the particle states are

proportional to the sum of the squares of the Ω 's of the nucleons. Then the total diagonal energy is given by

$$E_T \text{ (diag)} = \frac{\hbar^2}{2\mathcal{I}} \langle R^2 \rangle + C \sum_{i=1}^n \Omega_i^2. \quad (4)$$

The matrix elements of the Coriolis operator are (cf. ref. 36 or ref. 38)

$$H_{K,K+1}^I = -\frac{\hbar^2}{2\mathcal{I}} \{ [I(I+1) - K(K+1)] [j(j+1) - \Omega(\Omega+1)] \}^{1/2}. \quad (5)$$

We may now write the secular equation for the levels of spin I in our general nucleus. Expressing it in determinantal form, the diagonal elements are $[E_T(I,K) - W]$ where $E_T(I,K)$ is given by Eq. (4). The first off-diagonal elements, $H_{K,K+1}^I$, are given by Eq. (5); all other off-diagonal elements are zero. The order of the determinant is $(I + 1/2)$. For example, the secular equation for $I = 7/2$ and $j \geq 7/2$ is

$$\begin{vmatrix} E(7/2,1/2) - W & H_{1/2,3/2}^{7/2} & 0 & 0 \\ H_{1/2,3/2}^{7/2} & E(7/2,3/2) - W & H_{3/2,5/2}^{7/2} & 0 \\ 0 & H_{3/2,5/2}^{7/2} & E(7/2,5/2) - W & H_{5/2,7/2}^{7/2} \\ 0 & 0 & H_{5/2,7/2}^{7/2} & E(7/2,7/2) - W \end{vmatrix} = 0.$$

The roots of the secular equation give the energies of the perturbed levels of spin I . The complete perturbed rotational spectrum is obtained by solving the secular equation for each I .

The odd-mass deformed nuclei may be described approximately in terms of the model used here. Hence, the above development may be used to calculate the effect of the Coriolis interaction in these nuclei, but,

because this description is only approximate, the correspondence between the calculated spectra and the actual nuclear spectra cannot be expected to be quantitative.

Specifically, there are two major discrepancies between this model and actual nuclei. First, it has been implicitly assumed that there are no residual forces between nucleons (i.e., independent particle motion). If this were true, even-even nuclei should have excited particle states at approximately twice the excitation energy of the first excited particle state in the lower, neighboring odd-mass nuclei. These states have not been observed and their absence is associated with the pairing force between nucleons. The results of both Equations (2) and (5) will be affected by this configuration mixing.

Secondly, the assumption that the relative energies of the particle states are proportional to $\Sigma \Omega^2$ is valid only in the limit of small deformation. At the deformations necessary for rotational spectra the spacings will deviate from this approximation, and in some cases these deviations may be quite large.

Despite these rather serious approximations, spectra calculated in the manner described show clearly the major effects of the Coriolis interaction on the spacings of the levels of rotational bands. Sample spectra are shown in Figs. 14, 15, 16, 17, 18, and 19. These spectra are for $j = 13/2$, $\underline{n} = 1, 3, \text{ and } 5$ and $j = 15/2$, $\underline{n} = 1, 3, \text{ and } 5$, respectively. They have been calculated for $[\hbar^2/2 \mathfrak{I} C] = 0.05$; the energy scale is arbitrary. The levels on the left of each figure are the unmixed rotational levels obtained from Eq. (4). The position of these levels after the inclusion of the Coriolis interaction are shown on the right. Only the levels of the two lowest rotational bands are shown.

To simplify the calculation of these spectra only the interactions of the $K = 1/2, 3/2, \text{ and } 5/2$ rotational bands were considered for $\underline{n} = 1$ and 3; for $\underline{n} = 5$ the interaction of the $K = 7/2$ band was also included. The effect of the neglected interactions on the levels shown will be small and, if included, would not change the qualitative features of the spectra.

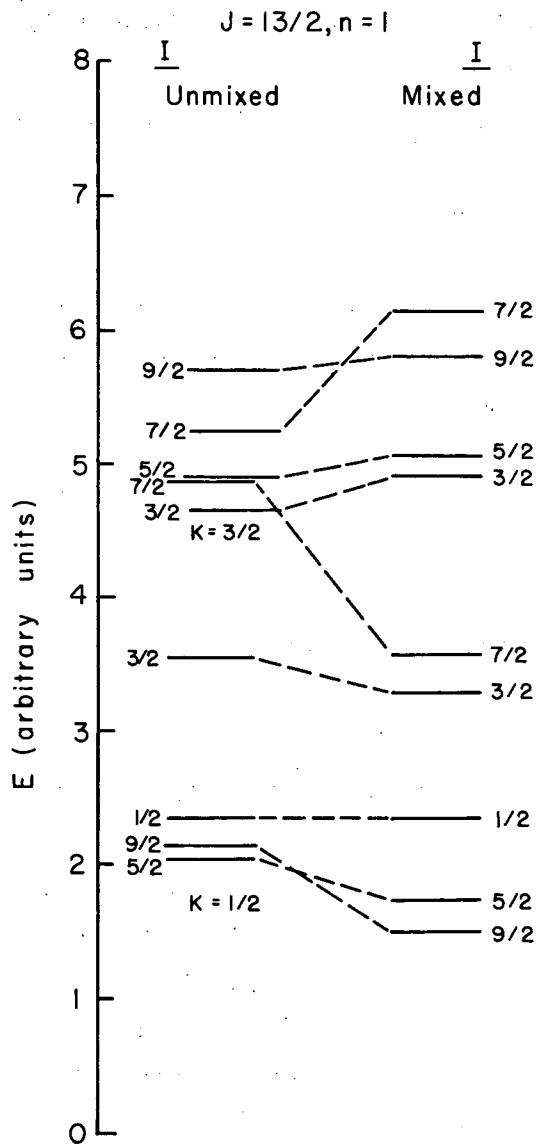
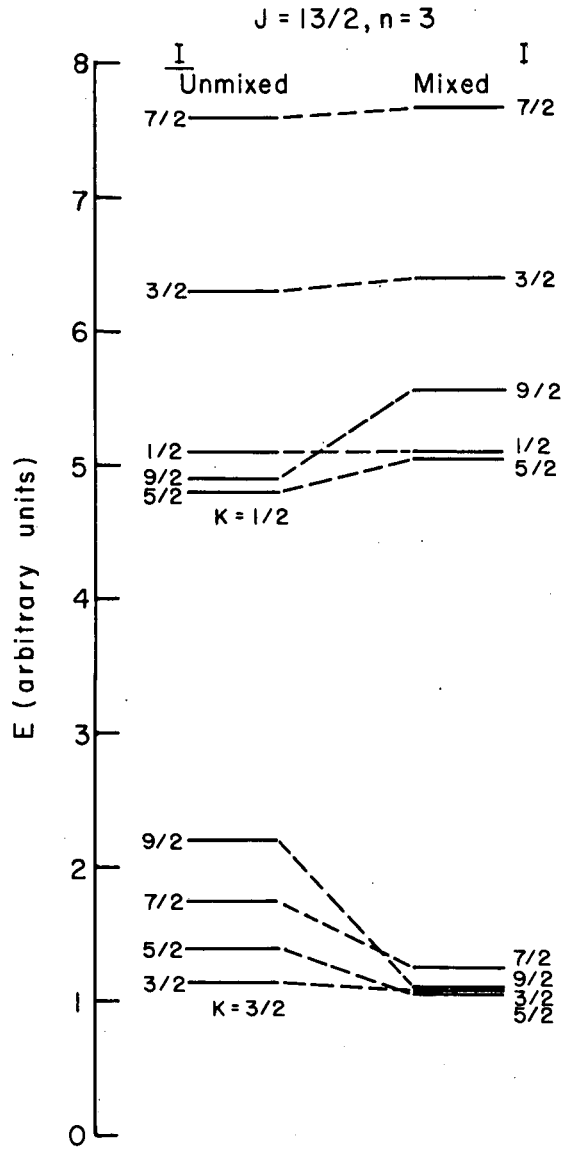
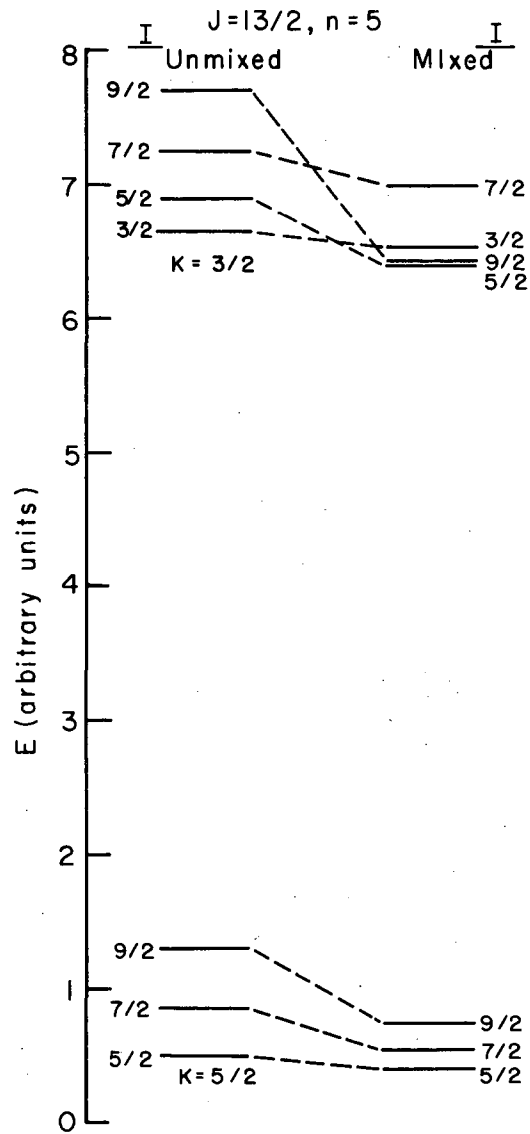


Fig. 14. Mixed rotational levels of a generalized nucleus with $j = 13/2, n = 1, \hbar^2/2 \mathfrak{I} C = 0.05$.



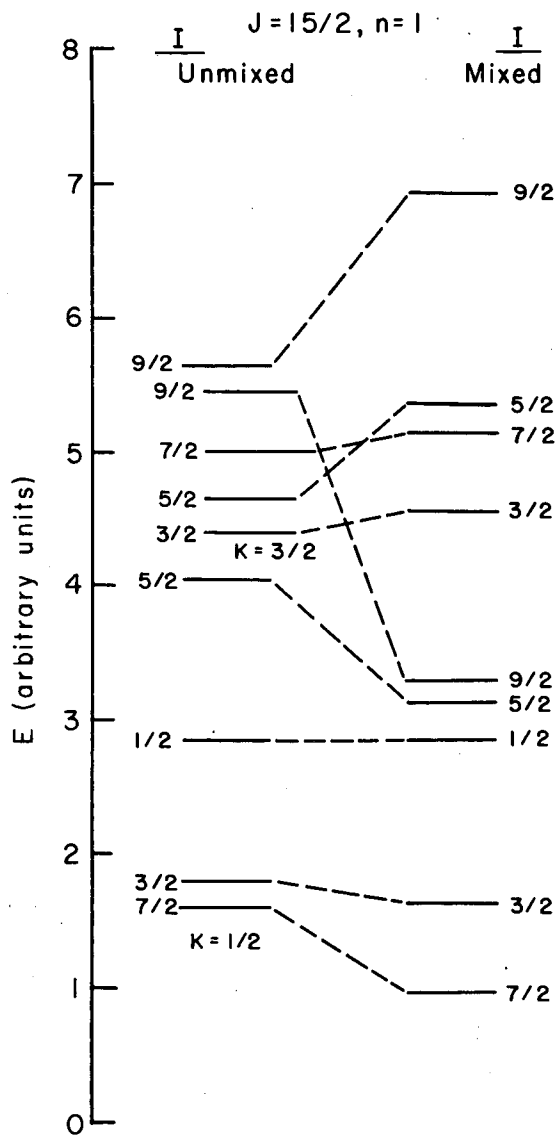
MU - 20272

Fig. 15. Mixed rotational levels of a generalized nucleus with $j = 13/2, n = 3, \hbar^2/2 \mathfrak{J} C = 0.05$.



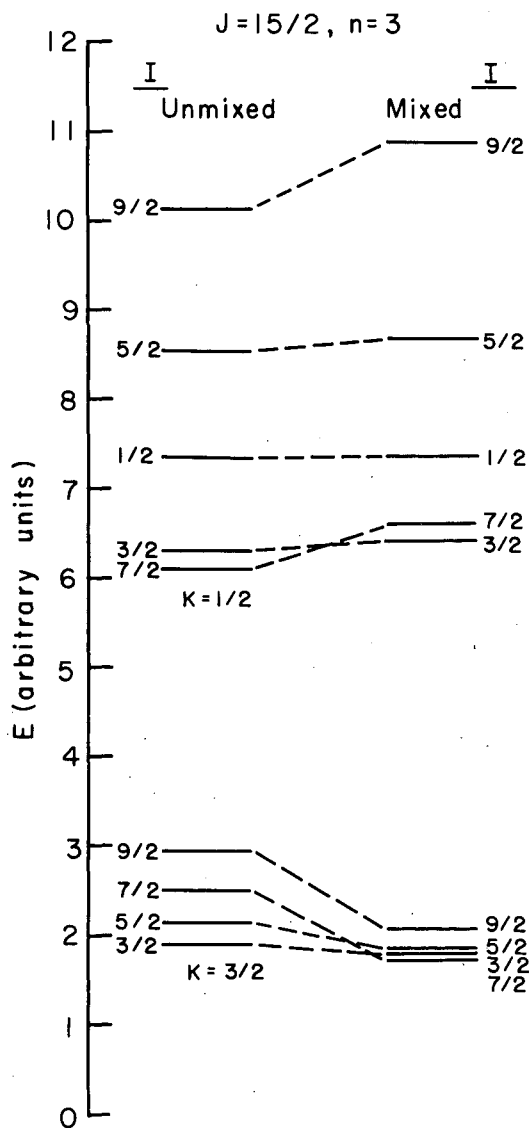
MU-20273

Fig. 16. Mixed rotational levels of a generalized nucleus with $j = 13/2, n = 5, \hbar^2/2 \approx C = 0.05$.



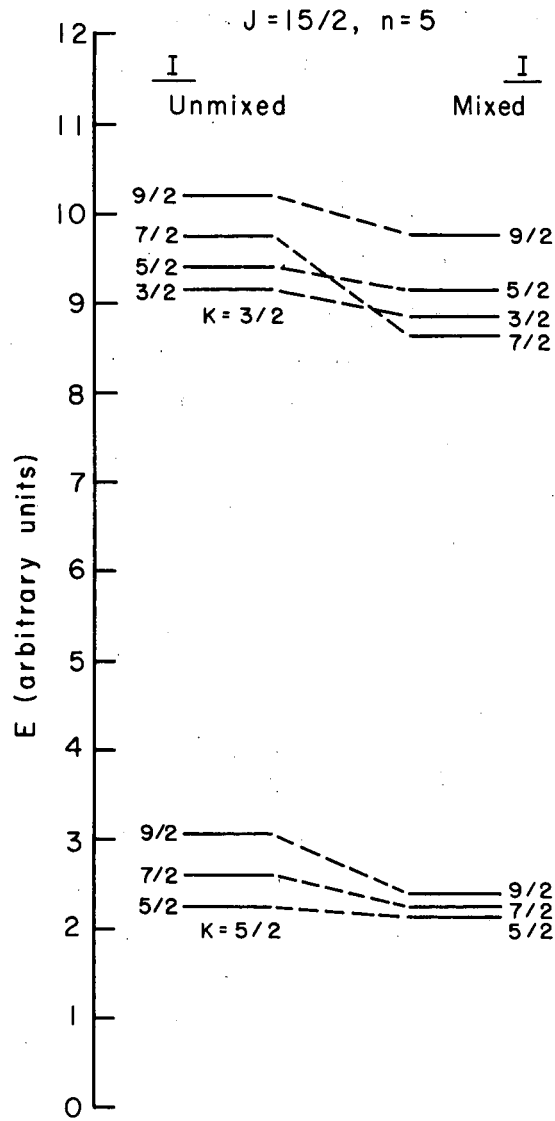
MU-20274

Fig. 17. Mixed rotational levels of a generalized nucleus with $j = 15/2, n = 1, \hbar^2/2 \mathfrak{S} C = 0.05$.



MU - 20275

Fig. 18. Mixed rotational levels of a generalized nucleus with $j = 15/2, n = 3, \kappa^2/2 \approx C = 0.05$.



MU-20276

Fig. 19. Mixed rotational levels of a generalized nucleus with $j = 15/2, n = 5, \hbar^2/2 \mathfrak{I} C = 0.05$.

The effects of the Coriolis interaction in actual nuclei seldom, if ever, will be as great as the effects shown here. In this sense these mixed spectra are unrealistic; they will, however, serve as graphic hyperboles.

The most striking effect illustrated by these spectra is the mutual distortion of the $K = 1/2$ and $3/2$ bands. For $j = 13/2$ the sign of the decoupling term of the $K = 1/2$ band is negative for $I = 1/2, 5/2, 9/2, \dots$; the sense of the mutual distortion for the $K = 1/2$ band lowest is shown in Fig. 14 and for the $K = 3/2$ band lowest in Fig. 15. For $j = 15/2$ the sign of the decoupling term is negative for $I = 3/2, 7/2, 11/2, \dots$; the sense of the mutual distortion for the $K = 1/2$ band lowest is shown in Fig. 17 and for the $K = 3/2$ band lowest in Fig. 18. For other values of j the mutual distortion of the $K = 1/2$ and $3/2$ bands will be similar to (but less pronounced than) one of the examples shown here. If $(j + 1/2)$ is an odd number, the appropriate examples will be those for $j = 13/2$; if $(j + 1/2)$ is an even number, the appropriate examples will be those for $j = 15/2$.

The second major effect of the Coriolis interaction is illustrated by the $K = 5/2$ bands in Figs. 16 and 19. This effect is the compression of these bands causing them to exhibit extremely large effective moments of inertia. If, for example, we assume that $\hbar^2/2 \mathfrak{I} = 10$ kev for the unmixed $K = 5/2$ band of Fig. 16, we find from the separation of the $I = 5/2$ and $7/2$ levels that $\hbar^2/2 \mathfrak{I} = 4$ kev for the mixed band. Furthermore, the $I = 9/2$ level is found to be at 68 kev rather than at 64 kev as predicted by the simple rotational formula. This is the discrepancy which, in the perturbation limit, is described by adding a positive $I^2 (I + 1)^2$ correction term to the simple rotational formula (see Introduction). The effect of the interaction on $K \geq 7/2$ bands should be similar to its effect on the $K = 5/2$ band.

It should be emphasized that the interacting rotational bands considered here are all based on particle states in which the odd nucleon is in orbitals of the same \vec{j} (but different Ω). If a nucleus has rotational bands based on particle states for which the odd nucleon is in orbitals of different \vec{j} , there will be no Coriolis interaction

between them if they have opposite parity; if the bands have the same parity, there usually will be an interaction between them but it will be relatively weak. In either case, however, each of these bands will be subject to interactions of the type described here.

THE CORIOLIS INTERACTION IN PROTACTINIUM-233 AND -231

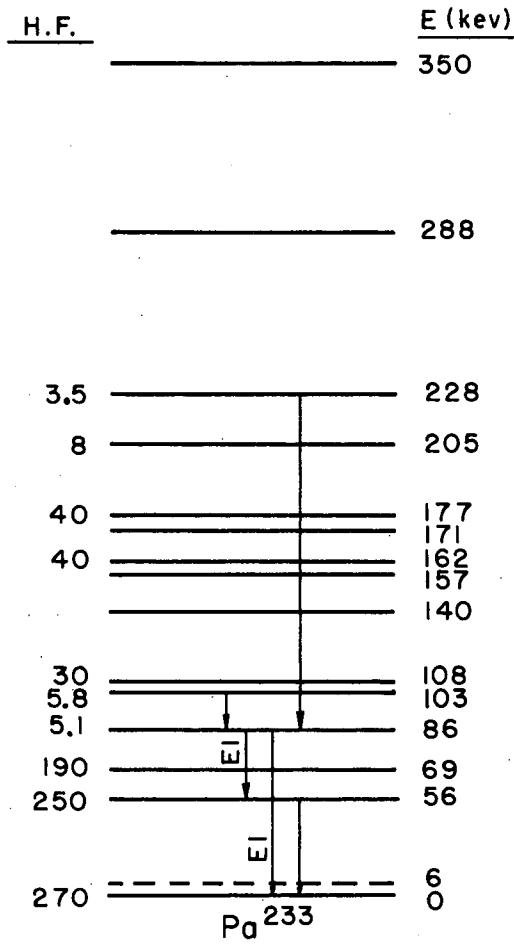
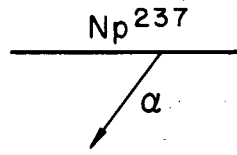
Stephens, Asaro, and Perlman⁴¹ have concluded that the apparent lack of rotational structure in the isotopes of actinium and protactinium is probably due to the presence of a large number of anomalous $K = 1/2$ rotational bands in this region and their effect through the Coriolis interaction on the nearby $K = 3/2$ (and in some cases $K = 5/2$) rotational bands. Using this conclusion, they have made Nilsson state assignments to the levels of these isotopes. Their assignments will be used as the basis of this discussion of the Coriolis interaction in Pa^{233} and Pa^{231} .

The levels of Pa^{233} populated by the alpha decay of Np^{237} are shown in Fig. 20.* The pertinent section of the Nilsson level diagram is given in Fig. 21. The level assignments of Stephens, et al. for Pa^{233} are:

- (1) the levels at 0, 6, 56, and 69 kev are, respectively, the $I = 3/2, 1/2, 7/2,$ and $5/2$ members of a rotational band based on the Nilsson level $1/2^- [530]$,
- (2) the level at 86 kev is the $5/2^+ [642]$ Nilsson level, and
- (3) the level at 205 kev is probably the $3/2^+ [651]$ level.

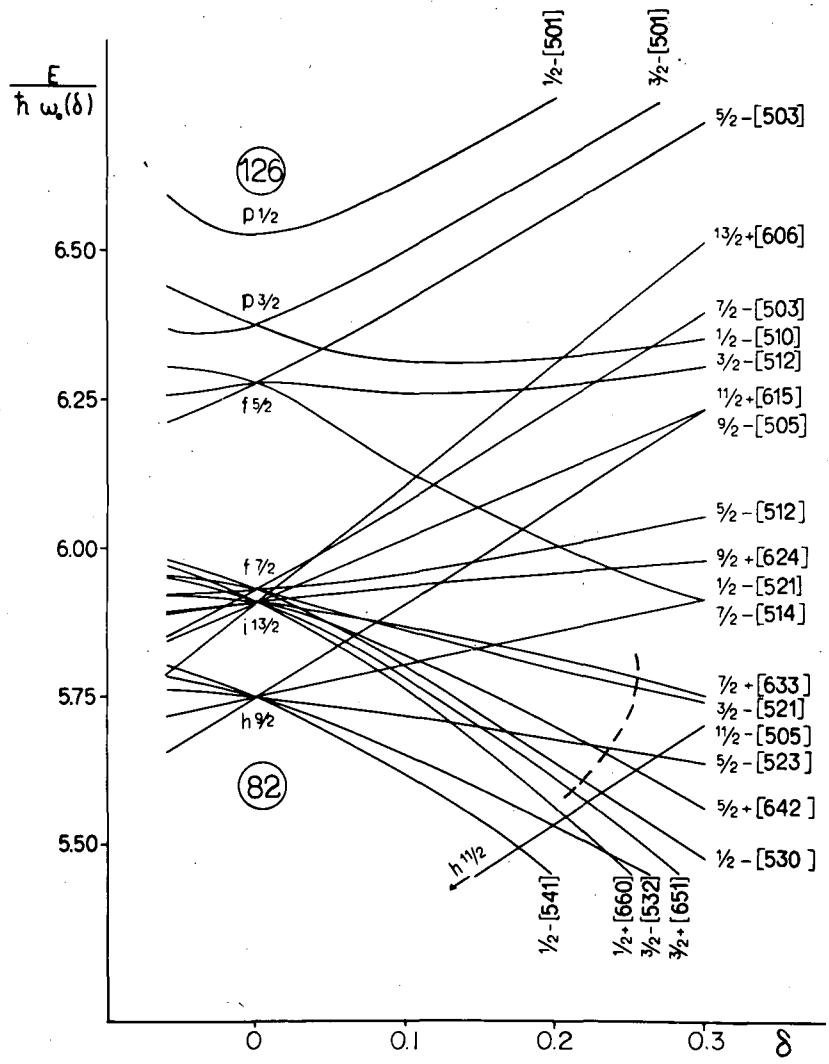
Mottelson and Nilsson⁴² have suggested the same assignments for these levels and, in addition, have suggested that the levels at 157 and 177

* These levels, with the exception of the 108-kev level, are taken from the compilation of Mottelson and Nilsson.⁴² The 108-kev level, the multipolarities of the 30- and 86-kev transitions, and the alpha-decay hindrance factors given here are from a private communication from Asaro, Perlman, and Stephens.



MU - 20277

Fig. 20. The energy levels of Pa^{233} .



MU-15745

Fig. 21. Nilsson level diagram for protons for $82 \leq Z \leq 126$. The abscissa is the nuclear deformation (prolate), and the ordinate gives the relative energy of the levels. The dashed line indicates very roughly the deformations of the heavy elements (Stephens, Asaro, and Perlman⁴¹).

keV are the $I = 11/2$ and $9/2$ members of the $1/2^-$ rotational band, the level at 103 keV is the $I = 7/2$ member of the $5/2^+$ [642] band, and the level at 228 keV is the $I = 5/2$ member of the $3/2^+$ [651] band.

The members of the rotational bands based on the $5/2^+$ [642] and $3/2^+$ [651] levels will be coupled by the Coriolis force.* In addition, the $1/2^+$ [660] and the $7/2^+$ [633] levels may lie nearby. Their rotational bands will be strongly coupled to the rotational bands of the $3/2^+$ [651] and $5/2^+$ [642] levels, respectively.

The experimental evidence tends to confirm the presence of a pronounced interaction of the type just outlined. First of all, the well-developed $1/2^-$ rotational band indicates that the nucleus has a stable spheroidal deformation; yet, there is no obvious rotational band based on the $5/2^+$ level at 86 keV (nor on the somewhat more tentatively assigned $3/2^+$ level at 205 keV). As suggested by Stephens, et al., the Coriolis interaction may account for this lack of apparent rotational structure. Secondly, if the level at 103 keV is the $I = 7/2$ member of the $5/2^+$ [642] rotational band, this band must have a very large moment of inertia. As noted before, one of the characteristic effects of the Coriolis interaction is an increase in the moment of inertia. Finally, the alpha-decay hindrance factors (see Fig. 20) indicate that the levels at 86 and 103 keV and the levels at 205 and 228 keV are populated by

*The strength of this coupling may be reduced since these particle states are formed in a different manner. The $5/2^+$ [642] state is formed by promoting the odd proton to this level from the $1/2^-$ [530] level while the $3/2^+$ [651] state is formed by promoting one of the paired protons in this level to the $1/2^-$ [530] level. Nominally, then, the $5/2^+$ [642] state has $5 \ 1_{13/2}$ protons and the $3/2^+$ [651] state has only $3 \ 1_{13/2}$ protons. Since the Coriolis operator is a single particle operator we would expect no interaction in the absence of configuration mixing. However, configuration mixing via the important pairing interaction will cause some coupling between these states and this coupling can produce a large effect since the energy separation of the interacting levels is extremely small.

avored alpha decay. Since the ground state of Np^{237} is the $5/2+$ [642] level (Stephens, et al.⁴¹) favored alpha decay to the 86- (and 103-) kev level is expected (this is actually one of the arguments used in assigning this level). Mottelson and Nilsson (MN, p. 56) suggest that the favored alpha decay to the levels at 205 and 228 kev may be explained as the result of Coriolis coupling between the $5/2+$ [642] and $3/2+$ [651] rotational bands.*

If, as the evidence suggests, we have here a group of rotational bands coupled by strong Coriolis interactions, it seems likely that some of the other levels shown in Fig. 20 are members of these bands but are not recognized as such because of their distorted energy spacings. Preliminary calculations by Stephens⁴³ indicated that this is the case. Consequently, we have made a more detailed study of the Coriolis interactions between the even parity rotational bands expected to be at relatively low energies in Pa^{233} .

Four interacting rotational bands have been considered here; these are the bands based on the $1/2+$ [660], $3/2+$ [651], $5/2+$ [642], and $7/2+$ [633] intrinsic states. The effect of the Coriolis interaction on the energies of their levels was computed by solving secular equations of the type given in the preceding section. The diagonal elements of these equations are the energies of the levels of the rotational bands in the absence of the Coriolis interaction. Five parameters, the position of one member of each rotational band and a moment of inertia (assumed to be the same for all bands), were used to specify these energies. The limiting value of $j + 1/2 = 7$ was used for the decoupling constant of the $1/2+$ band. The off-diagonal elements were assumed to have the dependence on I , j , and $K (= \Omega)$ given by equation (5) of the preceding section. The magnitude of these elements was allowed to vary by replacing $\hbar^2/2\mathcal{I}$ with a variable parameter k .

* A similar effect has been noted in the alpha decay of U^{235} (F. Asaro, private communication and MN, p. 12).

The set of calculated levels giving the best agreement with the experimental levels is shown in Fig. 22. A comparison of Figs. 20 and 22 shows the following correspondence (in energy) of levels.

<u>Experimental Energy</u>	<u>Calculated Energy</u>	<u>I of Calculated Level</u>
86 kev	87 kev	5/2
103	101	7/2
108	115	9/2
157*	155	11/2
171	173	13/2
205	205	3/2
228	224	5/2
288	292	7/2
350	354	13/2

Also, there is preliminary experimental evidence that the alpha group which populates the 288-kev level is complex⁴⁴ indicating that there may be a level corresponding to the $I = 9/2$ level predicted to be at 275 kev. Considering the approximations used in this calculation and the large interactions involved, the energy agreement shown here is quite good.

With the exception of the 86-kev level, the spins and parities of the levels shown in this comparison are not known experimentally. If the assignment of the ground state rotational band is correct, the 86-kev level must be $5/2+$; this agrees with the spin of the corresponding calculated level. The spins of the calculated levels corresponding to the experimental levels at 103, 205, and 228 kev agree with the assignments of Stephens, et al. and Mottelson and Nilsson. The identification of

* Mottelson and Nilsson (MN, p. 55) have tentatively assigned this level as the $I = 11/2$ member of the ground state rotational band. However, this assignment seems inconsistent with the relatively small alpha-decay hindrance factor which they have given for this level.

<u>I</u>	<u>E (kev)</u>
1/2	386
5/2	379
13/2	354
7/2	292
9/2	275
5/2	224
3/2	205
13/2	173
11/2	155
9/2	115
7/2	101
5/2	87
	0

MU - 20278

Fig. 22. The spectrum of mixed rotational levels calculated for Pa²³³.

the 108-keV level with the $I = 9/2$, 115-keV calculated level is clearly indicated by the absence of other levels in this energy region in both the experimental and calculated spectra; similarly, the possibly complex level at 288 keV must be identified with the calculated $I = 7/2$ and $9/2$ levels at 292 and 275 keV. The rather small alpha-decay hindrance factors for these levels (Fig. 20 and MN, p. 54) support these identifications, since the indicated spins predict that these levels will be populated by $L = 2$ (and higher) alpha waves. Since the energy agreement which we have found for other levels is of the order of a few keV and there are five levels in the experimental spectrum between 140 and 177 keV, the identification of the $I = 11/2$ and $13/2$ calculated levels at 155 and 173 keV with the particular levels shown in the comparison is rather uncertain. Because of the approximations used in obtaining the calculated spectrum, we cannot rule out the possibility that the 350-keV experimental level may be identified with either the $I = 5/2$ or $1/2$ levels shown at 379 and 380 keV in Fig. 22.

The agreement between experimental and calculated spectra very strongly suggests that the levels shown in the preceding comparison are members of mixed rotational bands. Yet, since we have used six parameters and the identification of at least three of the nine levels of our comparison are questionable, further evidence in support of this interpretation is needed. Unfortunately, there are not sufficient experimental data on the transitions between these levels to test this interpretation by a comparison of experimental and theoretical electromagnetic transition probabilities. However, additional evidence may be obtained from a more detailed analysis of the alpha-decay transition probabilities to the $I \leq 9/2$ levels and from a comparison of the probable Coriolis interactions in Pa^{233} and Pa^{231} .

The energy-independent, or reduced, alpha-decay transition probabilities to the different members of an unmixed rotational band are given by⁴⁵

$$P = P_0(Z, E) \sum_L C_L (I_i L K_i K_f - K_i | I_i L I_f K_f)^2. \quad (6)$$

P is the reduced transition probability to the level I_f, K_f ; $P_o(Z, E)$ is the reduced transition probability for unhindered alpha decay to this level, c_L is a constant characteristic of the particular decay and alpha wave of angular momentum L, and the quantity in parentheses is a Clebsch-Gordan coefficient. Since we are concerned with mixed rotational levels, we will have to use a modified form of this equation.

The wave functions of these mixed levels may be written in the form

$$\bar{\Psi}_u^I = a_u^{I,1/2} \psi^{I,1/2} + a_u^{I,3/2} \psi^{I,3/2} + a_u^{I,5/2} \psi^{I,5/2} + a_u^{I,7/2} \psi^{I,7/2}$$

$\psi^{I,K}$ is the wave function of the pure level I in the rotational band K. The coefficients $a_u^{I,K}$ measure the amount of $\psi^{I,K}$ in $\bar{\Psi}_u^I$ and may be evaluated from the off-diagonal matrix elements and the energy separation of the pure rotational levels; these coefficients for the levels of interest are given in Table VI. The index u numbers the mixed levels of spin I .

To reduce the number of parameters in this analysis we will neglect the contributions of $\psi^{I,1/2}$, $\psi^{I,7/2}$ and all alpha waves with $L > 2$ to the alpha-decay probabilities. Using these approximations the modified form of equation (6) is

$$P = P_o(Z, E) \sum_{L=0,2} [a_u^{I,5/2} b_L^{5/2} (I_i L K_i K_f - K_i | I_i L I_f K_f) + a_u^{I,3/2} b_L^{3/2} (I_i L K_i K_f - K_i | I_i L I_f K_f)]^2 \quad (6a)$$

where $b_L^K = \pm \sqrt{(c_L^K)^{1/2}}$.

The alpha-decay hindrance factors given in Fig. 20 are defined by

$$H. F. \equiv \frac{P_o(Z, E)}{P}$$

Table VI

Numerical Values of $a_u^{I,K}$ for Pa²³³

I;E (kev) of calc. level	$a_u^{I,1/2}$	$a_u^{I,3/2}$	$a_u^{I,5/2}$	$a_u^{I,7/2}$
5/2; 87	0.09	0.34	0.94	----
7/2; 101	0.07	0.42	0.90	0.10
9/2; 115	0.24	0.52	0.81	0.13
11/2; 155	0.10	0.51	0.84	0.16
13/2; 173	0.39	0.58	0.70	0.15
3/2; 205	0.13	0.99	----	----
5/2; 224	0.44	0.83	-0.35	----
9/2; 275	0.69	0.50	-0.51	-0.11
7/2; 292	0.21	0.88	-0.43	-0.08
13/2; 354	0.74	0.27	-0.59	-0.18

Assuming that the spins of the experimental levels are those of the corresponding calculated levels, we have evaluated $(b_0^{5/2})^2$, $b_2^{5/2}$, and $b_2^{3/2}$ from the hindrance factors of the 86-, 103-, and 205-kev levels. They are

$$\begin{aligned} (b_0^{5/2})^2 &= c_0^{5/2} = 0.08 \\ b_2^{5/2} &= 0.89 \\ b_2^{3/2} &= -0.67. \end{aligned}$$

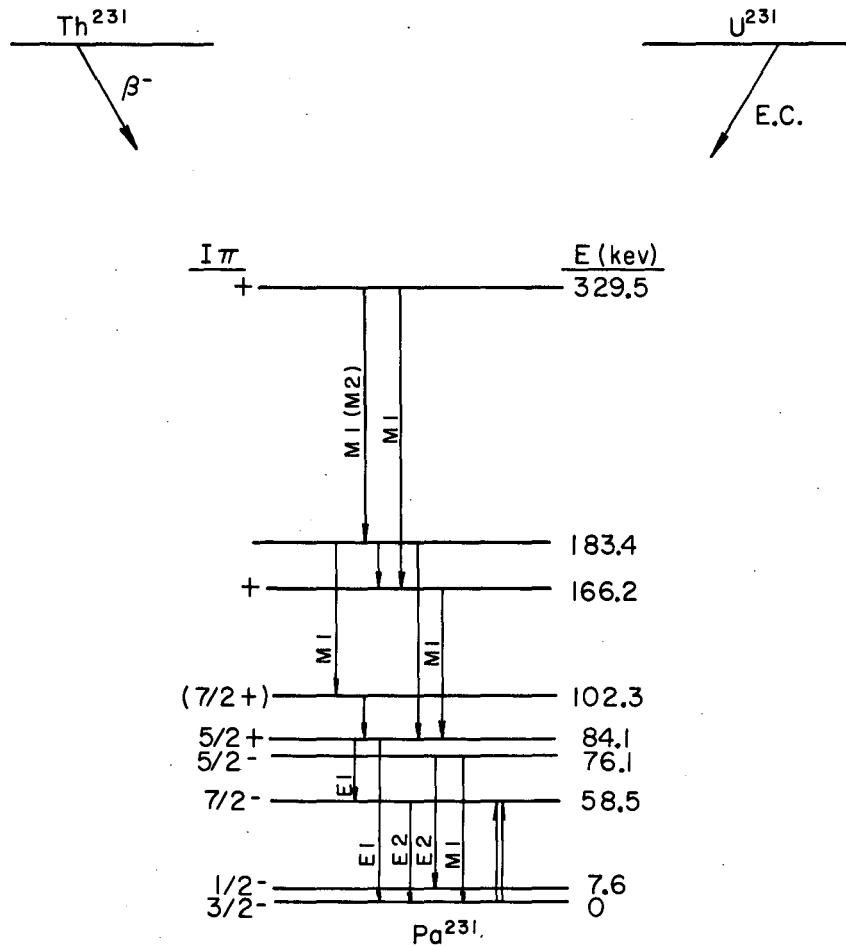
Mathematically, the choice of the relative sign of $b_2^{5/2}$ and $b_2^{3/2}$ is arbitrary. However, $b_2^{5/2}$ describes decay taking place between levels based on the same Nilsson state and it would be expected that $|b_2^{5/2}| > |b_2^{3/2}|$. The choice of opposite sign satisfies this condition; the choice of like sign does not.

We are now able to give an explanation of the anomalously small hindrance factor of the 228-kev level. Normally, this hindrance factor should be larger than that of the 103-kev level since the latter level is populated by favored alpha decay. However, the mixing of levels by the Coriolis interaction causes an interference between the $L = 2$ waves for $K = 3/2$ and $5/2$. This interference enhances the population of the 228-kev level and reduces the population of the 103-kev level. The quantitative extent of this effect is given quite well by the b_L^K values above; the calculated hindrance factor of the 228-kev level* is 3.3 compared to the empirical hindrance factor of 3.5. Also, the predicted hindrance factor of 21 for the 108-kev level is in fair agreement with the empirical value of 30.

While the interference effect considered here explains the anomalously small hindrance factor of the 228-kev level in an extremely gratifying manner, there must be other important factors influencing the alpha decay of Np^{237} . The interference between alpha waves should also enhance the population of the 288-kev level and the predicted hindrance factor for this level is comparable to that of the 228-kev level; yet, empirically, the hindrance factor of the former level is about four times that of the latter (MN, p. 54). In addition, the value found for $c_0^{5/2}$ indicates that the $L = 0$ alpha wave is very highly hindered. Since there is only one $L = 0$ wave, this hindrance cannot be due to an interference effect.

Figure 23 shows the spectrum of Pa^{231} determined by Hollander, Stephens, Asaro, and Perlman⁴⁶ from a study of the beta decay of Th^{231} and the electron-capture decay of U^{231} . The levels at 0, 7.6, 58.5, and

*The wave function corresponding to this level has a sizeable admixture of $\psi^{5/2,1/2}$ which we have neglected in this analysis. If in addition to $c_0^{5/2}$, $b_2^{5/2}$, and $b_2^{3/2}$, we evaluate $b_2^{1/2}$ from the hindrance factors of the 86-, 103-, 205-, and 228-kev levels, we find that $b_2^{1/2}$ is small and that the $L = 2$ waves for $K = 3/2$ and $5/2$ are the dominant factors in the alpha decay as the analysis above assumes.



MU-20279

Fig. 23. The energy level scheme of Pa^{231} .

76.1 keV have been assigned as the $I = 3/2, 1/2, 7/2,$ and $5/2$ members of a rotational band based on the $1/2^-$ [530] Nilsson level; the 84.1-keV level has been assigned as the $5/2^+$ [642] Nilsson level; the 102.3- and 166.2-keV levels are, respectively, probably the $I = 7/2$ member of the $5/2^+$ [642] rotational band and the $3/2^+$ [651] Nilsson level (Stephens, et al.⁴¹ and Hollander, et al.⁴⁶).

These assignments are the same as those made in Pa^{233} and imply that there is also a strong Coriolis interaction in Pa^{231} . Normally, we could not obtain evidence for the presence of this interaction by fitting a calculated spectrum to the experimental spectrum since there are only five even parity levels known in Pa^{231} and we have required at least six parameters to specify the elements of the secular equations. In this case, however, the parameter values are not arbitrary but should be very nearly the same as those of Pa^{233} . Then, if we can fit calculated levels to the experimental levels of Pa^{231} using parameter values similar to those used to obtain the spectrum of Fig. 22, this fit will provide evidence for the presence of the Coriolis interaction in both Pa^{233} and Pa^{231} by demonstrating the internal consistency of the present interpretation of their very similar spectra.

In addition to the spin assignments given above we have assumed, in analogy to Pa^{233} , that the spin of the 183-keV level is $5/2$. This limits the possible spins of the 330-keV level to $3/2$ and $5/2$, since this level decays by M1 transitions* to the 166- and 183-keV levels. The most probable source of the level is the $1/2^+$ [660] rotational band. Since the $I = 5/2$ member of this band should lie lower than the $I = 3/2$ member we have assigned a spin of $5/2$ to the 330-keV level.**

* While the experimental data do not preclude the possibility that the 146-keV transition is M2 we have disregarded this choice because of the assumed even parity of the 183-keV level.

** This assignment is quite tenuous since there is experimental evidence that the intensity of the β^- transition to this level is inconsistent with its being a member of the $1/2^+$ [660] rotational band (J. M. Hollander, private communication).

A calculated spectrum was fitted, both in energy and assumed spin, to the experimental spectrum of Pa²³¹. As in the case of Pa²³³, the decoupling constant of the K = 1/2 rotational band was taken to be $j + 1/2$, and the off-diagonal elements followed the form of Eq. (5) with $\hbar^2/2 \mathcal{S}$ replaced by the variable \underline{k} . The parameter values used for this fit are compared in Table VII to those used to obtain the spectrum of Fig. 22. This comparison clearly demonstrates the internal consistency for which we were looking and thus gives evidence of the Coriolis interactions in both nuclei.

Table VII

Parameters for Calculation of Mixed Spectra		
Parameter	Pa ²³³ (Fig. 22)	Pa ²³¹
$\hbar^2/2 \mathcal{S}$	5.5 kev	5.9 kev
$E_{1/2,1/2}$	380	326.4
$E_{3/2,3/2}$	210	171.8
$E_{5/2,5/2}$	105	104.7
$E_{7/2,7/2}$	605	605
		$\sqrt{12}$ for $H_{1/2,3/2}$
\underline{k}	$\sqrt{11}$	$\sqrt{8.7}$ for $H_{3/2,5/2}$
		$\sqrt{11}$ for $H_{5/2,7/2}$

In fitting a spectrum of mixed rotational levels to the experimental levels of Pa²³³ the parameters were permitted to vary freely over fairly wide ranges of values. For this reason the parameter values used to calculate the spectrum of Fig. 22 are somewhat arbitrary and their plausibility should be checked in the light of available external evidence. This plausibility check will, of course, also be applicable to the parameter values used to fit the levels of Pa²³¹.

At present, it is not possible to make a very rigorous check on the assumed energy separations of the unmixed rotational bands; however, the plausibility of these separations can be demonstrated. The energies of the intrinsic states upon which the rotational bands are based may be calculated from the Nilsson wave functions, but these generally are not quantitatively correct. We may note, though, that the relative separations of the $I = K$ members of the positive parity rotational bands are similar to those predicted by the Nilsson wave functions for the corresponding intrinsic states. (Since the $3/2+$ [651] intrinsic state is a "hole" state, i.e., it is formed by the promotion of a paired proton from the $3/2+$ [651] level to the $1/2-$ [530] level, the relative separation which should be compared to the separation of the $3/2+$ [651] and $5/2+$ [642] intrinsic states is proportional to $E_{3/2,3/2} + E_{5/2,5/2}$, not $E_{3/2,3/2} - E_{5/2,5/2}$.)

We may also compare these assumed energy separations to the energy separations between these intrinsic states observed in other heavy nuclei. This comparison is given in Table VIII. The intrinsic state assignments used in making this comparison are those of Stephens, et al.⁴¹; with the exception of the $5/2+$ [642] -- $7/2+$ [633] separation in Am^{243} , the assignment of at least one of the two intrinsic states involved in each separation is somewhat uncertain. The observed separations given here have been corrected, where appropriate, for the appearance of the intrinsic states as "hole" states. The assumed position of the $1/2+$ [660] level cannot be checked in this manner, since this level has not been identified in any of the heavy nuclei; this level has a very profound influence on the mixed rotational levels. Although the value of this comparison is limited by the uncertainties in the intrinsic state assignments and the inability to check the assumed position of the $1/2+$ [660] level, the comparison clearly shows that the magnitudes of the assumed separations are comparable to those of the observed separations. The combination of these considerations of the relative and absolute magnitudes of the assumed energy separations indicates that these separations are quite plausible.

Table VIII

Energy Separations Between Intrinsic States		
Intrinsic States	E_{assumed} (kev)	E_{observed} (kev)
1/2- [530] -- 3/2+ [651]	210 in Pa ²³³	330 in Ac ²²⁷
1/2- [530] -- 5/2+ [642]	105	267 Np ²³⁷
		353 Am ²³⁹
		274 Am ²⁴¹
		181 Am ²⁴³
1/2- [530] -- 7/2+ [633]	605	730 Am ²⁴³
5/2+ [642] -- 7/2+ [633]	500	549 Am ²⁴³
		393 Bk ²⁴⁹

Rotational bands based on the 5/2+ [642] intrinsic state have been identified in Np²³⁷ and Np²³⁹. Their moments of inertia will give us a check on the moment of inertia which we have used for this rotational band in Pa²³³. The value of $\hbar^2/2\mathcal{I} = 5.5$ kev which we have used for Pa²³³ corresponds to a moment of inertia 15 and 20% smaller than the moments of Np²³⁷ ($\hbar^2/2\mathcal{I} = 4.7$ kev) and Np²³⁹ ($\hbar^2/2\mathcal{I} = 4.4$ kev). A difference of this sort is to be expected for two reasons. First, the deformation of Pa²³³ should be smaller than the deformations of Np²³⁷ and Np²³⁹; there will be a decrease in the moment of inertia associated with this decrease in deformation. Secondly, the moments which we are comparing are not completely equivalent. The moments given for the neptunium isotopes are experimental and include the total effect of the Coriolis force on the odd proton. The moment used for the Pa²³³ rotational band is effectively the moment this band would have in the absence of those Coriolis interactions considered in these calculations. Consequently, the moment of inertia which we have used for Pa²³³ should

appear to be smaller than the moments of the neptunium isotopes.* We may conclude then that the moment of inertia used for the 5/2+ [642] rotational band in Pa²³³ is quite reasonable. The smaller moment of inertia used for this band in Pa²³¹ may indicate a smaller deformation for this nucleus or it may represent only an artificial change arising from the approximations used in our calculations.

In order to keep the number of parameters at a minimum we have assumed that the moments of inertia of all the interacting bands are identical. While there is no reason to expect this assumption to be exactly true, it should still provide a reasonable first approximation, since the odd proton has the same angular momentum in each of the intrinsic states upon which these rotational bands are based.**

Equation (5) for the matrix elements of the Coriolis operator assumes that j is a good quantum number or that

$$\langle x_{\Omega+1} | j_+ | x_{\Omega} \rangle = [j (j + 1) - \Omega (\Omega + 1)]^{1/2} .$$

Since the matrix elements $\langle x_{\Omega+1} | j_+ | x_{\Omega} \rangle$ can be evaluated from the Nilsson wave functions we should be able to check the validity of Eq. (5) for Pa²³³ (and Pa²³¹). Mottelson and Nilsson (MN, p. 84) have assumed a deformation corresponding to $\eta = 4.8$ for the ground state configuration of Pa²³³. The values of $\langle x_{\Omega+1} | j_+ | x_{\Omega} \rangle$ obtained from the Nilsson wave functions for $\eta = 4$ and 6 are given in Table IX along

*The difference between the moment of inertia used for Pa²³³ and the moments of the neptunium isotopes due to this effect should be about equal to the contribution made to the moment of inertia by the Coriolis interaction between the 5/2+ [642] and 7/2+ [633] rotational bands.

**This argument is oversimplified. The situation with regard to these moments is quite complex and will not be considered in detail here.

with the corresponding values of $[j(j+1) - \Omega(\Omega+1)]^{1/2}$. A comparison of these values indicates that the matrix elements given by Eq. (5) should be approximately correct for Pa²³³. Nevertheless, it was found that the matrix elements given by Eq. (5) were too large and, consequently, the variable \underline{k} was introduced in place of $\hbar^2/2\mathcal{S}$. The value of \underline{k} (i.e., $\sqrt{11}$ kev) used to obtain the spectrum of Fig. 22 corresponds to a 40% reduction of the matrix elements of Eq. (5). A spectrum very nearly identical to that of Fig. 22 is obtained if $\underline{k} = \sqrt{12}$ kev is used in conjunction with the values of $\langle \chi_{\Omega+1} | j_+ | \chi_{\Omega} \rangle$ for $\eta = 4$. This discrepancy is not sufficient to cast doubt upon the plausibility of our matrix elements since single-particle wave functions often give very poor values for matrix elements. For example, Grayson and Nordheim⁴⁷ compared a large number of single-particle theoretical beta-decay matrix elements to experimental beta-decay matrix elements and found the theoretical values to be consistently much greater (of the order of a factor of 10) than the experimental values.

Table IX

Theoretical Matrix Elements			
Coupled States	$\langle \chi_{\Omega+1} j_+ \chi_{\Omega} \rangle$		$[j(j+1) - \Omega(\Omega+1)]^{1/2}$
	$\eta = 4$	$\eta = 6$	
1/2+ [660]; 3/2+ [651]	6.65	6.21	6.93
3/2+ [651]; 5/2+ [642]	6.45	6.21	6.71
5/2+ [642]; 7/2+ [633]	6.16	6.01	6.33

To minimize the number of parameters needed to calculate a spectrum comparable to that of Pa²³³ we required \underline{k} to be the same for all of the matrix elements. It was noted previously, however, that $H_{3/2,5/2}$ might be relatively smaller than the other matrix elements. In fitting the levels of Pa²³¹ we permitted \underline{k} to assume different values for each set of matrix elements. These values of \underline{k} (see Table VII) indicate some weakening of the

interaction between the $K = 3/2$ and $5/2$ rotational bands; the extent of this weakening is not large, though, and the requirement of constant k may be regarded as a reasonable approximation.

We assume that the decoupling constant of the $1/2+$ [660] rotational band was $j + 1/2 = 7$. For $\eta = 4$ and 6 the values of this constant given by the Nilsson wave functions are 6.68 and 6.15. This comparison would seem to indicate that our approximation is reasonably accurate, but, since the Nilsson wave functions gave values of $\langle \chi_{\Omega+1} | j_{\pm} | \chi_{\Omega} \rangle$ which were too large, the value of this comparison is somewhat questionable. However, it is the only available check of the accuracy of this approximation.

The evidence presented in this section, i.e., the agreement of the levels of Fig. 22 with the experimental levels of Pa^{233} , the analysis of the alpha decay of Np^{237} , the internal consistence of this interpretation in Pa^{233} and Pa^{231} , and the plausibility of the parameter values used in obtaining calculated spectra, makes it seem rather certain that many of the levels of Pa^{233} and Pa^{231} are members of rotational bands mixed by a strong Coriolis interaction. Yet, an experimental determination of the spins of these levels and extensive data on the electromagnetic transitions between them would still be very useful both to confirm the presence of this interaction and to permit a more flexible analysis of its effects.

ACKNOWLEDGMENT

The author is indebted to Drs. M. I. Kalkstein, C. J. Gallagher, Jr., D. Q. Strominger, and K. T. Faler for assistance in various phases of the experimental portion of this investigation, to Drs. F. S. Stephens, Jr., F. Asaro, J. M. Hollander, and Professor I. Perlman for making their data on the protactinium isotopes available prior to publication, and to Miss Carolyn Lovejoy for guiding this manuscript through the preparations for its printing.

The author is grateful to the Health Chemistry department of the Lawrence Radiation Laboratory for arranging the neutron irradiations, transporting targets, and assisting in the handling of radioactive materials, and to W. B. Jones and the crew of the Berkeley 60-inch cyclotron for carrying out the alpha-particle irradiations necessary for this study.

The greatest measure of appreciation is due to Professor John O. Rasmussen, under whose direction this study was made.

This work was performed under the auspices of the United States Atomic Energy Commission.

REFERENCES

1. Strominger, Hollander, and Seaborg, *Revs. Modern Phys.* 30, 585 (1958); R. G. Wille and R. W. Fink, *Phys. Rev.* 112, 1950 (1958).
2. V. Kistiakowsky Fischer, A Study of the Isotopes of Promethium (Thesis), UCRL-1629, January 1952; *Phys. Rev.* 87, 859 (1952).
3. W. W. Meinke, Chemical Procedures Used in Bombardment Work at Berkeley, UCRL-432, August 1949.
4. Thompson, Harvey, Choppin, and Seaborg, *J. Am. Chem. Soc.* 76, 6229 (1954).
5. A. Ghiorso and A. E. Larsh, in Chemistry Division Quarterly Report, UCRL-2647, July 1954.
6. Manufactured by the Pacific Electro-Nuclear Company, Culver City, California.
7. M. I. Kalkstein and J. M. Hollander, A Survey of Counting Efficiencies for a 1-1/2-Inch Diameter by 1-Inch High Sodium Iodide (Thallium-Activated) Crystal, UCRL-2764, October 1954.
8. R. L. Heath, Scintillation Spectrometry Gamma-Ray Catalogue, IDO-16408, July 1957.
9. P. Axel, Escape Peak Corrections to Gamma-Ray Intensity Measurements Made with Sodium Iodide Crystals, BNL 271 (T-44), September 1953; *Rev. Sci. Instr.* 25, 391 (1954).
10. G. D. O'Kelley and J. L. Olsen, A Ring-Focussed, Long Magnetic Lens Beta-Ray Spectrometer, California Research and Development Company Report MTA-38, May 1954.

11. G. D. O'Kelley, The Spectrometric Determination of Some Beta-Particle and Conversion-Electron Energies (Thesis), UCRL-1243, June 1951.
12. W. G. Smith, I. Neutron-Deficient Isotopes in the Noble Metal Region. II. Conversion-Electron Spectra of Some Heavy Elements (Thesis), UCRL-2974, June 1955; W. G. Smith and J. M. Hollander, Phys. Rev. 101, 746 (1956).
13. Caporiacco, Ferrero, and Mandò, to be published.
14. Pohm, Lewis, Talboy, and Jensen, Phys. Rev. 95, 1523 (1954).
15. H. Brysk and M. E. Rose, Theoretical Results of Orbital Capture, ORNL-1830, January 1955.
16. G. W. Grodstein, X-Ray Attenuation Coefficients from 10 kev to 100 Mev, NBS Circular 583, 1957.
17. C. M. Davisson and R. D. Evans, Revs. Modern Phys. 24, 79 (1952).
18. Reported in Appendix IX of X-Rays in Theory and Experiment, A. H. Compton and S. K. Allison, Van Nostrand, New York (1935).
19. E. Feenberg and G. Trigg, Revs. Modern Phys. 22, 399 (1950).
20. Grace, Johnson, Scurlock, and Taylor, Phil. Mag. 3, 456 (1958).
21. M. E. Rose and R. K. Osborn, Phys. Rev. 93, 1326 (1954).
22. P. F. Zweifel, Phys. Rev. 107, 329 (1957).
23. Perlman, Welker, and Wolfsberg, Phys. Rev. 110, 381 (1958).

24. B. S. Dzhelepov and L. K. Peker, Decay Schemes of Radioactive Nuclei, Academy of Sciences of the U. S. S. R. Press, Moscow (1958).
25. Strominger, Höllander, and Seaborg, *Revs. Modern Phys.* 30, 585 (1958).
26. V. K. Fischer, *Phys. Rev.* 96, 1549 (1954).
27. Rutledge, Cork, and Burson, *Phys. Rev.* 86, 775 (1952).
28. The time-to-pulse-height converter used in this study is a modification of the circuit described by Weber, Johnstone, and Cranberg, *Rev. Sci. Instr.* 27, 166 (1956).
29. L. A. Sliv and I. M. Band, Coefficients of Internal Conversion of Gamma Radiation, (Academy of Sciences, U. S. S. R.). Translation issued in United States as Reports 57, ICCKI (1956) and 58, ICCLI (1958), University of Illinois, Urbana, Illinois.
30. G. S. Bogle and H. E. D. Scovil, *Proc. Phys. Soc.* 65A, 368 (1952).
31. K. Murakawa, *Phys. Rev.* 93, 1232 (1954).
32. E. Feenberg, Shell Theory of the Nucleus, Princeton University Press, Princeton (1955), Ch. V.
33. S. B. Burson and L. C. Schmid, Physics Division Summary Report, ANL-5955, January 1959.
34. S. B. Burson, private communication.
35. A. Bohr and B. Mottelson, *Dan. Mat. Fys. Medd.* 27, No. 16 (1953).
36. A. Bohr, *Dan. Mat. Fys. Medd.* 26, No. 14 (1952).

37. J. O. Rasmussen, Concerning K-Mixing in Bohr-Mottelson States of Spheroidal Nuclei, UCRL-3149, September 1955 (unpublished).
38. A. K. Kerman, Dan. Mat. Fys. Medd. 30, No. 15 (1956).
39. O. Prior, Arkiv f. Fysik 14, 451 (1958).
40. S. G. Nilsson, Dan. Mat. Fys. Medd. 29, No. 16 (1955).
41. Stephens, Asaro, and Perlman, Phys. Rev. 113, 212 (1959).
42. B. R. Mottelson and S. G. Nilsson, Mat. Fys. Skr. Dan. Vid. Selsk. 1, No. 8 (1959). Referred to in text as MN.
43. F. S. Stephens, Jr., private communication.
44. F. Asaro, private communication.
45. Bohr, Fröman and Mottelson, Dan. Mat. Fys. Medd. 29, No. 10 (1955).
46. Hollander, Stephens, Asaro, and Perlman, to be published.
47. W. C. Grayson, Jr., and L. W. Nordheim, Phys. Rev. 102, 1093 (1956).

This report was prepared as an account of Government sponsored work. Neither the United States, nor the Commission, nor any person acting on behalf of the Commission:

- A. Makes any warranty or representation, expressed or implied, with respect to the accuracy, completeness, or usefulness of the information contained in this report, or that the use of any information, apparatus, method, or process disclosed in this report may not infringe privately owned rights; or
- B. Assumes any liabilities with respect to the use of, or for damages resulting from the use of any information, apparatus, method, or process disclosed in this report.

As used in the above, "person acting on behalf of the Commission" includes any employee or contractor of the Commission, or employee of such contractor, to the extent that such employee or contractor of the Commission, or employee of such contractor prepares, disseminates, or provides access to, any information pursuant to his employment or contract with the Commission, or his employment with such contractor.